# Anisomycin, a JNK and p38 activator, suppresses cell–cell junction formation in 2D cultures of K38 mouse keratinocyte cells and reduces claudin-7 expression, with an increase of paracellular permeability in 3D cultures

**Misaki Nikaido [a], Takahito Otani [b], Norio Kitagawa [b], Kayoko Ogata[b], Hiroshi Iida [c], Hisashi Anan [a], Tetsuichiro Inai *, [b]**

[a] Department of Odontology, Fukuoka Dental College, 2-15-1 Tamura, Sawara-ku, Fukuoka 814-0175, Japan

[b] Department of Morphological Biology, Fukuoka Dental College, 2-15-1 Tamura, Sawara-ku, Fukuoka 814-0175, Japan

[c] Laboratory of Zoology, Graduate School of Agriculture, Kyushu University, 6-10-1 Hakozaki, Higashi-ku, Fukuoka 812-8581, Japan

**Corresponding author:** Tetsuichiro Inai, D.D.S., Ph.D., Department of Morphological Biology, Fukuoka Dental College, 2-15-1 Tamura, Sawara-ku, Fukuoka 814-0193, Japan.
Tel.: +81-92-801-0411 Ext. 683, fax: +81-92-801-4909.
E-mail: tinaitj@college.fdcnet.ac.jp

**Abstract**

Keratinocytes in the oral mucosal epithelium, which is a non-keratinized stratified epithelium, are exposed to various stimuli from the oral cavity. JNK and p38 are stress-activated mitogen-activated protein kinases (MAPKs) that are phosphorylated by various stimuli and are involved in the assembly and disassembly of tight junctions (TJs) in keratinocytes. Therefore, we investigated the effects of stress-activated MAPKs on TJs in a mouse keratinocyte cell line (K38) during cell–cell junction formation in two-dimensional (2D) cultures or stratification to form non-keratinized epithelium in 3D cultures. In 2D cultures, calcium induced zipper-like staining for ZO-1 at 2 h and string-like staining for ZO-1 at 12 h, which indicated immature and mature cell–cell junctions, respectively. Anisomycin (AM), a JNK and p38 activator, inhibited formation of string-like staining for ZO-1, whereas inhibition of JNK, but not p38, after AM treatment restored string-like staining for ZO-1, although claudins (CLDNs) 4, 6, and 7 did not completely colocalize to ZO-1-positive sites. In 3D cultures, AM treatment for 2 weeks activated only p38, suppressed flattening of the superficial cells, removed CLDN7 from ZO-1-positive spots on the surface of 3D cultures, which represent TJs, and decreased transepithelial electrical resistance. Thus, short-term AM treatment inhibited maturation of cell–cell junctions by JNK, but not p38, activation. p38 activation by long-term AM treatment affected morphology of stratified structures and paracellular permeability, which was increased by CLDN7 removal from TJs. Various chronic stimuli that activate stress-activated MAPKs may weaken the keratinocyte barrier and be involved in TJ-related diseases.

**Key words:** c-Jun $NH_2$-terminal protein kinase (JNK); p38 mitogen-activated protein kinase (MAPK); Tight junction; Claudin; Keratinocyte; Three-dimensional culture.

## Introduction

The human epidermis is a keratinized stratified epithelium that consists of basal, spinous, granular, and cornified layers. Keratin (K) 14 and K5 are localized to basal cells (Moll et al. 2008; Torma 2011), while K10 and K1 appear in spinous cells (Kim et al. 2002; Torma 2011). The epithelia in the human oral cavity, esophagus, cornea, and vagina are non-keratinized and stratified, and consist of basal, intermediate, and superficial layers (Al Yassin and Toner 1977); all keratinocytes in these layers possess a nucleus. In contrast to humans, in mice and rats, the epithelia in the oral cavity, esophagus, and forestomach are keratinized (Barrett et al. 1998; Jones and Klein 2013).

Three-dimensional (3D) keratinocyte cultures on collagen gels containing dermal fibroblasts are widely used as a skin analog, and 3D cultures of keratinocytes on the filters of cell culture inserts are used as a model for a keratinized stratified epithelium (epidermis) (Frankart et al. 2012; Poumay et al. 2004; Seo et al. 2016) . However, there are only a few studies that used 3D cultures as a model for a non-keratinized stratified epithelium: mouse and human esophageal keratinocytes (Kalabis et al. 2012) or an immortalized human oral keratinocyte cell line, OKF6/TERT2 (Dongari-Bagtzoglou and Kashleva 2006), on collagen gels with fibroblasts and human bronchial epithelial cells on filter inserts (Oshima et al. 2011). Although bronchial epithelial cells form a pseudostratified epithelium *in vivo*, they formed non-keratinized stratified epithelium in the presence of 0.3 nM retinoic acid *in vitro* (Oshima et al. 2011). Similarly, K38, a murine keratinocyte cell line derived from epidermis, formed non-keratinized stratified epithelium-like structures using recently established 3D culture methods (Seo et al. 2016).

Tight junctions (TJ) regulate paracellular permeability; they comprise a multi-protein complex composed of transmembrane and cytosolic plaque proteins such as claudin (CLDN), occludin, tricellulin, ZO-1, ZO-2, and ZO-3. CLDN1 expression in TJ-free fibroblasts reconstituted TJ strands observed by freeze-fracture electron microscopy, indicating that

CLDNs form the backbone of TJ strands (Furuse et al. 1998). In the epidermis, TJs are formed in the second of three granular layers (Furuse et al. 2002; Kubo et al. 2009; Tsuruta et al. 2002). However, TJ proteins, including CLDNs 1, 4, 6, 7, 11, 12, 17, and 18, show distinct localizations from the basal layer to the granular layer in the epidermis (Brandner et al. 2002; Brandner et al. 2006; Brandner et al. 2003; Furuse et al. 2002; Haftek et al. 2011; Igawa et al. 2011; Morita et al. 2004; Troy et al. 2005). CLDN6 was detected in the periderm of mouse embryo, but not in the granular layer of newborn mouse epidermis (Morita et al. 2002). In the cornea, cldns1, 4, and 7 were broadly distributed from the basal to the superficial layers, but occludin and ZO-1 were restricted to the superficial cells (Ban et al. 2003; Nakatsukasa et al. 2010; Takaoka et al. 2007; Yoshida et al. 2009). With some variations, similar localization patterns for these TJ proteins were reported in the esophagus (Oshima et al. 2011; Oshima et al. 2012) and the oral mucosa (Babkair et al. 2016).

Mitogen-activated protein kinases (MAPKs) are a family of serine-threonine kinases that are involved in modulating cellular responses (Bogoyevitch and Court 2004; Hagemann and Blank 2001; Pearson et al. 2001; Schaeffer and Weber 1999). MAPKs include extracellular signal-regulated kinase-1 and -2 (ERK1/2), c-Jun $NH_2$-terminal kinases (JNK1/2/3), p38 (p38α/β/γ/δ), ERK3/4, ERK5, and ERK7/8 in mammalian cells (Kyriakis and Avruch 2001). JNK1 and JNK2 are ubiquitously expressed, while JNK3 is localized to the brain, heart, and testes (Davis 2000).

Keratinocytes in the oral mucosal epithelium are exposed to various stimuli from the surface including thermal, pH, and osmotic stresses, substances derived from bacteria and food, diagnostic or therapeutic radiation, and signals from connective tissues including cytokines. JNK and p38 are known as stress-activated MAPKs phosphorylated by various stimuli and are involved in the assembly and disassembly of TJs in keratinocytes (Siljamaki et al. 2014) and in other cells (Kojima et al. 2010; Naydenov et al. 2009). Consistent with these

observations, HaCaT cells (a normal human epidermal keratinocyte cell line) formed TJs when treated with SP600125 (an inhibitor of JNK) (Aono and Hirai 2008; Kitagawa et al. 2014). Furthermore, SP600125-treated HaCaT cells stopped expressing K5 and accumulated occludin at cell–cell contacts, suggesting that these cells underwent differentiation (Kitagawa et al. 2014). The short-term effect of stress-activated MAPKs on TJs was examined in 2D culture of HaCaT cells (Minakami et al. 2015). However, the long-term effects of stress-activated MAPKs on TJs in 3D keratinocyte cultures have not been thoroughly investigated to date.

In this study, we investigated the short-term (within 12 h) and long-term (2 weeks) effects of stress-activated MAPKs activated by AM on TJs in 2D and 3D cultures of K38. 2D cultures are used to investigate the short-term effects of AM on cell–cell junction formation induced by calcium. K38 3D cultures, which reconstituted non-keratinized stratified epithelium-like multilayers, were used to examine the long-term effects of AM on morphology, expression, and localization of TJ proteins, and paracellular permeability in the course of stratification.

## Materials and methods

### *Antibodies*

Primary antibodies used in this study were as follows: mouse anti-CLDN4, anti-occludin, and anti-ZO-1 antibodies and rabbit anti-CLDN1 and anti-ZO-1 (Mid) antibodies (Zymed, South San Francisco, CA, USA); rabbit anti-CLDN6 and anti-CLDN7 antibodies (IBL, Takasaki, Japan); mouse anti-phospho (P)-JNK (G9) and anti-JNK1 (2C6) antibodies and rabbit anti-P-ERK (p44/42 MAPK), anti-ERK, anti-JNK2 (56G8), anti-JNK (#9252), anti-P-p38 (D3F9), anti-p38 (D13E1), anti-p38α, anti-p38β (C28C2), anti-p38γ, anti-p38δ (10A8) and anti-E-cadherin antibodies (Cell Signaling Technology, San Diego, CA, USA); mouse

anti-K4 (clone 5H5) and rabbit anti-actin antibodies (Sigma-Aldrich, Saint Louis, MO, USA); rabbit anti-loricrin (LOR) antibody (BioLegend, San Diego, CA, USA).

***Cell culture medium***

FAD medium (Biochrom GmbH, Berlin, Germany) consisted of DMEM/HAM's F12 (3.5:1.1), 50 μM $CaCl_2$, and 4.5 g/L D-glucose, and was supplemented with 10% Chelex 100-treated fetal bovine serum (FBS), 0.18 mM adenine (Sigma-Aldrich), 0.5 μg/mL hydrocortisone (Sigma-Aldrich), 5 μg/mL insulin (Life Technologies, Carlsbad, CA, USA), $10^{-10}$ M cholera toxin (Sigma-Aldrich), 10 ng/mL epidermal growth factor (EGF; Sigma-Aldrich), 2 mM L-glutamine (Nacalai Tesque, Kyoto, Japan), and 1 mM sodium pyruvate (Wako, Osaka, Japan). Calcium in the serum was removed by treating 500 mL FBS (HyClone, South Logan, UT, USA) with 20 g of Chelex 100 (Bio-Rad Laboratories, Hercules, CA, USA) (Lichti et al. 2008). EpiLife medium (Gibco, Grand Island, NY, USA) was supplemented with human keratinocyte growth supplement (Gibco) consisting of 0.2% bovine pituitary extract, 5 μg/mL bovine insulin, 0.18 μg/mL hydrocortisone, 5 μg/mL bovine transferrin, and 0.2 ng/mL human EGF. CnT-PR (CELLnTEC, Bern, Switzerland) and EpiLife are low calcium growth mediums, containing 70 μM and 60 μM $CaCl_2$, respectively. For 3D culture (Seo et al. 2016), cells were grown in each growth medium supplemented with 1.2 mM calcium chloride (Nacalai Tesque), 10 ng/mL human keratinocyte growth factor (KGF; PeproTech, Rocky Hill, NJ, USA), and 0.283 mM L-ascorbic acid phosphate magnesium salt *n*-hydrate (APM; Wako, Osaka, Japan), a stable derivative of ascorbic acid.

***2D and 3D cell culture***

The murine epidermal keratinocyte cell lines, COCA (Segrelles et al. 2011) and K38 (Reichelt and Haase 2010; Vollmers et al. 2012), originating from the back skin of adult

C57BL/DBA mice and neonatal BALB/c mouse skin and grown in CnT-PR and FAD medium, respectively, were purchased from ECACC (Salisbury, UK). Adult human epidermal keratinocytes (HEKa) (Gibco) were grown in EpiLife medium. For 3D culture, keratinocytes (HEKa, COCA, and K38; $7.5 \times 10^5$ cells/mL) were seeded in each low calcium growth medium into Merck Millipore cell culture inserts (0.4 μm polycarbonate filter, 12 mm diameter; Darmstadt, Germany) in 24-well plates. Each insert and each well contained 0.4 mL cell suspension ($3.0 \times 10^5$ cells) and 0.6 mL medium. Cells were grown for 1–2 days until they reached 100% confluence. The growth medium inside and outside of the insert was replaced with 3D high calcium medium and cells were cultured for 16–24 h to form intercellular adhesion structures. Then, up to 6 inserts were transferred to a 60-mm culture dish containing 3.2 mL 3D medium and airlifted cultures were established by removing the 3D medium in the inserts. The surfaces within the inserts were kept dry following airlift by removing excess 3D medium in the inserts. The medium was changed every 2 days and the air-liquid interface culture was maintained for up to 3 weeks.

CMT93 cells derived from mouse rectum carcinoma were obtained from ECACC, and CMT93-II cells were subcloned from CMT93 cells (Inai et al. 2008). MDCK II Tet-Off cells stably transfected with a Tet-Off regulatory plasmid were purchased from Clontech (Palo Alto, CA, USA). MDCK II Tet-Off cells and CMT93-II cells were grown in DMEM medium supplemented with 10% FBS, 2 mM glutamine, 100 U/ml penicillin, and 100 μg/ml streptomycin (Gibco). These cells were used to examine the specifications of antibodies used in this study by immunoblotting (Supplementary Fig. 1) and immunofluorescence staining (Supplementary Fig. 2).

### *Immunofluorescence microscopy*

For 2D cultures, K38 cells were seeded at a density of $1.0 \times 10^4$ cells/well in the wells (6 mm

diameter) of 10-well glass slides printed with highly water-repellent marks (catalog number TF1006; Matsunami Glass Ind. Ltd., Osaka, Japan). The next day, when the cells reached confluence, they were treated with vehicle, AM, or AM plus SB202190 (Sigma-Aldrich), BIR796 (Cayman Chemical, Ann Arbor, MI, USA), or SP600125 (Sigma-Aldrich) at the indicated concentrations and time points in the presence of 1.2 mM calcium. For 3D cultures, cells were cultured in 3D medium containing vehicle or AM (30, 50, or 100 nM) for 2 weeks. A stock solution of AM was prepared by dissolving it in dimethyl sulfoxide (DMSO) at concentration of 100 μM. SB202190, BIRB 796, and SP600125 are inhibitors of p38α/β, p38α/β/γ/δ, and JNK, respectively, and stock solutions in DMSO were prepared at concentrations of 20 mM, 10 mM, and 20 mM, respectively. Cells were fixed with 1% paraformaldehyde in PBS for 10 min. For 3D cultures, filters with cultured keratinocytes were fixed with 1% paraformaldehyde in PBS for 1 h at 4°C, washed in PBS and cut away from the inserts. The filters with cells were sequentially soaked in 10%, 20%, and 30% sucrose in PBS at 4°C for 1–3 h each, and then embedded in OCT compound (Sakura Finetek Japan, Tokyo, Japan). Cryosections (5 μm) were cut and mounted onto glass slides. Some sections were stained with HE. Cells in the wells of glass slides or cryosections were washed in PBS and incubated in 0.2% Triton-X 100 in PBS for 15 min for permeabilization. Subsequently, the sections were washed in PBS, and then incubated with 1% bovine serum albumin in PBS (BSA-PBS) for 15–30 min to block nonspecific binding. They were incubated with primary

antibodies diluted in BSA-PBS for 1 h in a moist chamber. As controls for immunofluorescence, BSA-PBS was used in place of the primary antibodies; the results are shown in Supplementary Fig. 3. The following primary antibodies were used: rabbit anti-CLDN1 (1:100), anti-CLDN6 (1:100), anti-CLDN7 (1:100), anti-ZO-1 (1:200), anti-E-cadherin (1:100) and anti-LOR (1:100), and mouse anti-CLDN4 (1:200), anti-occludin (1:50), anti-ZO-1 (1:1,000) and anti-K4 (1:100). After rinsing 4X in PBS, the sections were incubated with anti-mouse or anti-rabbit immunoglobulin (Ig) conjugated with either Alexa 488 or Alexa 568 (Molecular Probes, Eugene, OR, USA) at a 1:400 dilution in BSA-PBS for 30 min in the dark. The sections were then washed 4X in PBS and mounted in Vectashield mounting medium containing 4', 6-diamidino-2-phenylindole (DAPI) (Vector Laboratories, Burlingame, CA, USA). The images were obtained by sequentially scanning the specimen to prevent bleed-through using a LSM710 confocal laser scanning microscope with the ZEN 2010 software (Carl Zeiss, Oberkochen, Germany). The system settings were as follows: (1) objective lens: Zeiss Plan-Apochromat 63×/1.40 Oil DIC M27; fluorescence settings for DAPI: Diode 405-30 laser (405 nm) 4.0%, Channel (Ch) 1, pinhole 67.2 μm (1.0 μm section), filter 415–479 nm; Alexa 488: Argon laser (488 nm) 5.0%, Ch 1, pinhole 68.5 μm (1.0 μm section), filter 492–545 nm; Alexa 568: HeNe 543 laser (543 nm) 26.0%, Ch 2, pinhole 64.9μm (1.0 μm section), filter 555–812 nm; beam splitters: MBS: MBS488/543/633, MBS_InVis: MBS-405; and image size: 512 pixel (134.7μm) x 512 pixel (134.7μm), pixel

size=0.26 μm. Using auto exposure and range indicator, the master gain, digital offset (basically 0.00), and digital gain (basically 1.00–1.24) were determined. Images of the HE-stained sections were acquired using an Olympus BX51 microscope (Olympus Corporation, Tokyo, Japan) with an olympus objective lens (Ach, 60x/0.80) and an interlace scan CCD camera (Olympus DP12, 3.24 megapixel, 2048 x 1536 pixel resolution).

***Gel electrophoresis and immunoblot analysis***

Confluent cells cultured in 12-well plates or 3D-cultured cells in inserts were treated with vehicle (0.2% DMSO) or AM (Sigma-Aldrich) at the indicated concentrations and time points. Cells were washed with ice-cold PBS and lysed in 0.2 mL lysis buffer [62.5 mM Tris, pH 6.8, 2% sodium dodecyl sulfate (SDS), 10% glycerol, 5% 2-mercaptoethanol, and 0.002% bromophenol blue] containing protease inhibitor cocktail (Sigma-Aldrich) and phosphatase inhibitor cocktail (Nacalai Tesque). Cell lysates (5 μL per lane) were fractionated by SDS-polyacrylamide gel electrophoresis (PAGE) and then transferred onto polyvinylidene difluoride (PVDF) membranes. Precision Plus protein dual color standards (Bio-Rad Laboratories) were used to calculate the size of the detected bands. The membranes were incubated with Blocking One (Nacalai Tesque) for 1 h and then with primary antibodies (listed below) overnight at 4°C. Primary antibodies were diluted at 1:1000, except for anti-actin antibody (1:2000), with Tris buffered saline (TBS) [20 mM Tris (pH 7.6) and 137 mM NaCl] containing 5% Blocking One. After washing with TBS containing 0.1% Tween 20 (T-TBS), membranes were incubated with horseradish peroxidase (HRP)-conjugated anti-rabbit or anti-mouse Ig (1:2000) (GE Healthcare UK Ltd, Buckinghamshire, England) for 1 h. They were then washed with T-TBS and the bands were detected using Luminata Forte Western HRP substrate (Millipore, Billerica, MA, USA). Some membranes were reprobed after

stripping primary and secondary antibodies with stripping buffer [62.5 mM Tris (pH 6.7), 2% SDS, and 100 mM 2-mercaptoethanol] at 50°C for 30 min.

### *Measurement of transepithelial electrical resistance (TER)*

Two weeks after airlift, cell culture inserts were transferred into a 24-well plate. FAD medium containing 1.2 mM calcium was added to the inserts (0.4 mL) and wells (0.6 mL). TER was measured with a Millicell ERS-2 epithelial voltohmmeter (Millipore). After measurement of TER, filters with cultured keratinocytes were processed for immunofluorescence microscopy, HE staining, or immunoblot analysis. The TER values were calculated by subtracting the contribution of the bare filter and medium and multiplying it by the surface area of the filter. All experiments were performed twice in triplicate.

### *Statistical analysis*

All data are expressed as the mean ± standard error of mean (SEM). Statistical differences between groups were determined by the two-sided Welch's *t*- test. $P < 0.05$ was considered statistically significant.

## Results

### *Characterization of 3D culture of K38 and COCA cells*

In 3D cultures, HE staining showed that K38 and COCA cells formed non-keratinized and keratinized stratified squamous epithelium-like structures, respectively (Fig. 1A). The uppermost layer of K38 3D cultures at 1, 2, and 3 weeks consisted of flattened cells with nucleus and no obvious stratum corneum which should be stained pink with eosin (Fig. 1A, a–c). In contrast to K38, COCA cells formed keratinized multilayers at 1 week, but the stratum corneum developed a loosely packed appearance at 3 weeks compared to 1 and 2

weeks (Fig, 1A, d–f). While the suprabasal cells in K38 3D cultures expressed K4 (Fig. 1B, a), which is expressed in suprabasal cells in non-keratinized oral epithelium *in vivo*, COCA 3D cultures expressed LOR in cells just below the stratum corneum (Fig. 1B, b), corresponding to granular cells in keratinized epidermis *in vivo*. Specificity of antibodies against K4 and LOR was supported by immunolocalization of K4 and LOR in 3D cultures of K38 and COCA (Fig. 1B). In 2D monolayers cultured with 1.2 mM calcium, ERK and JNK1 were detected in all 3 types of keratinocytes by immunoblot analysis (Fig. 1C). Very weak JNK2 signals were detected in COCA and K38 cells. While COCA and K38 cells expressed p38α and p38γ, HEKa cells expressed p38α, p38β, and p38δ. HEKa and COCA cells expressed CLDNs 1 and 4, while K38 cells expressed CLDNs 1, 4, 6, and 7 proteins. In this study, we used the K38 cell line as a model system for non-keratinized stratified squamous epithelium.

***JNK and/or p38 inhibited cell–cell junction formation in K38 2D cultures***

We examined effects of AM, which activates both p38 and JNK, on the localization of CLDN4 and ZO-1 during the formation of cell–cell junctions induced by 1.2 mM calcium for 12 h (Fig. 2). Before addition of calcium, weak signals for CLDN4 and ZO-1 were detected in some cell–cell contacts and cytoplasm (Fig. 2a–c). In the absence of AM (Fig. 2d–l), dotted or zipper-like staining for CLDN4 and ZO-1 was detected in cell–cell contacts at 2 h (Fig. 2d–f), gradually replaced with straight and thin string-like staining for CLDN4 and ZO-1 at 6 h (Fig. 2g–i), and completely replaced at 12 h (Fig. 2j–l). Some zipper-like staining for ZO-1 was negative for CLDN4 (arrowheads in Fig. 2 d–i), suggesting that ZO-1 was first recruited to cell–cell contacts and followed by CLDN4. In the presence of AM (Fig. 2m–u), string-like staining for ZO-1 and CLDN4 appeared slowly with time compared to the control, and zipper-like staining remained at 12 h. Zipper-like staining for ZO-1 and either CLDNs 4, 6, or

7 were still detected in some cell–cell contacts up to 24 h (Supplementary Fig. 4). CLDN1 was detected only in a small number of cell–cell contacts in the control, and was not affected by AM treatment at 24 h (Supplementary Fig. 4). Therefore, we further examined the short-term effects of AM at 12 h, but did not examine localization of CLDN1.

***JNK, but not p38, inhibited cell–cell junction formation in K38 2D cultures***

Because AM phosphorylated both p38 and JNK, we attempted to inhibit one of them using SB202190, BIRB 796 or SP600125. Immunoblot analysis (Fig. 3) showed that AM transiently phosphorylated both p38 and JNK at 0.5 h but not at 12 h. AM plus BIRB 796, but not AM plus SB202190, inhibited phosphorylation of p38 and the upper band of JNK but did not affect that of the lower band of JNK at 0.5 h. The result is consistent because K38 expressed p38α and p38γ (Fig. 1C). AM plus SP600125 inhibited phosphorylation of the upper and lower bands of JNK and left p38 phosphorylated at 0.5 h. In the control, the lower band of ERK was highly phosphorylated at 0.5 h, compared to the upper band. After treatment with AM, phosphorylation of the upper and lower bands disappeared and decreased at 0.5 h, respectively. Phosphorylation of both bands was reduced by AM plus either SB202190 or SP600125 treatment at 0.5 h, but was not altered by AM plus BIRB 796 treatment at 0.5 h. In the control, phosphorylation of the lower band of ERK reduced to the level of the upper band at 12 h. There was no difference in phosphorylation levels of ERK at 12 h in case of the control, and after treatment with AM and AM plus either SB202190 , BIRB 796, or SP600125.

We next examined the localization of ZO-1 and either CLDN4 (Fig. 4), CLDN6 (Fig 5), or CLDN7 (Fig. 6) 12 h after addition of calcium in the presence of either vehicle, AM, AM plus SB202190, AM plus BIRB 796, or AM plus SP600125. In the control, all cell–cell contacts had a string-like appearance and were positive for both ZO-1 and CLDN4 (Fig. 4a–

c). As shown in Fig. 2, 12 h AM treatment (Fig. 4d–f) delayed formation of string-like staining for both ZO-1 and CLDN4 (arrows), leaving zipper-like staining for either ZO-1 (small arrowheads) or ZO-1 plus CLDN4. AM plus SB202190 (Fig. 4g–i) and AM plus BIRB 796 (Fig. 4j–l) did not induce formation of string-like staining, suggesting it was inhibited by activation of both p38γ and JNK or solely JNK. In contrast, AM plus SP600125 (Fig. 4m–o) induced formation of string-like staining, suggesting that inhibition of JNK activation restored formation of the string-like staining despite activation of both p38α and p38γ. Occasionally, string-like staining without CLDN4 was observed (large arrowheads in Fig. 4m–o) when treated with AM plus SP600125. Similar results were obtained when stained with ZO-1 and CLDN6 (Fig. 5) or ZO-1 and CLDN7 (Fig. 6). However, several differences were found for CLDNs 6 and 7, compared to CLDN4. AM (Fig. 5d–f), AM plus SB202190 (Fig. g–i), and AM plus BIRB 796 (Fig. 5j–l) treatments clearly decreased CLDN6 signal compared to the control (Fig. 5a–c). Although AM plus SP600125 (Fig. 5m–o) restored string-like staining for ZO-1, CLDN6 was partly recruited to cell–cell contacts and some areas were positive only for ZO-1 (large arrowheads in Fig. 5). In the control (Fig. 6a–c), CLDN7 was also localized in lateral plasma membranes as a fine dotted appearance in addition to the uppermost region of the lateral plasma membrane, where CLDN7 and ZO-1 were colocalized as a string-like appearance. AM (Fig. 6d–f), AM plus SB202190 (Fig. 6g–i), and AM plus BIRB 796 (Fig. 6j–l) did not restore string-like staining for ZO-1. Treatment with AM plus SB202190 or BIRB 796 slightly decreased CLDN7 signal. AM plus SP600125 (Fig. 6m–o) restored string-like staining for ZO-1. However, CLDN7 was not recruited to all the ZO-1 string-like staining (large arrowheads in Fig. 6m–o), although CLDN7 was detected in the lateral plasma membrane.

***Activation of p38 by long-term AM treatment in 3D cultures decreased CLDN7 and TER***

We further examined the long-term effects of AM for 2 weeks in 3D cultures of K38. Morphological analysis by HE staining showed that the superficial cells were flattened in control (Fig. 7A, a). Flattening of the superficial cells was inhibited by 30 and 50 nM AM but stratification itself was not inhibited (Fig. 7A, b, c). E-cadherin staining of cell–cell borders revealed several layers of flattened cells on the surface of control 3D cultures (arrowhead in Fig. 7B, a). The superficial cells were not flattened (arrowhead in Fig. 7B, b) when treated with 50 nM AM. To examine the barrier function of TJs in 3D cultures, TER was measured. TER was reduced by ~ 30% by 50 nM AM but not by 30 nM AM (Fig. 7C). Immunoblot analysis showed that p38 was activated by 50 nM AM compared to the control (Fig. 7D). JNK and ERK were not activated by 50 nM AM. Treatment with 50 nM AM increased CLDN1 and especially CLDN6, while it decreased CLDN4, ZO-1, E-cadherin, and CLDN7 (Fig. 7D). We did not detect occludin by immunoblot analysis.

In control 3D cultures, ZO-1-positive spots, which appear in cross sectional views of TJs, were observed in the first and second, and occasionally the third, layers from the surface in 3D cultures (Fig. 8A, a, d, g, j, m). ZO-1 was also localized at cell–cell borders in layers deeper from the surface. CLDN1 was not detected at ZO-1-positive spots on the surface (arrowheads in Fig. 8A, a–c) but was observed in the cytoplasm (Fig. 8A, b). CLDNs 4 (Fig. 8A, d–f) and 7 (Fig. 8A, j–l) were detected at ZO-1-positive spots (arrows) as well as cell–cell borders. CLDN6 was detected at some ZO-1-positive spots (arrows in Fig. 8A, g–i) but not at cell–cell borders (arrowheads in Fig. 8A, g–i). Occludin colocalized at ZO-1-positive spots (arrows in Fig. 8A, m–o) but not at cell–cell borders (Fig. 8A, m–o).

In AM-treated 3D cultures, cytoplasmic staining for CLDN1 was slightly increased (Fig. 8B, b). CLDN4 staining was not affected by AM (Fig. 8B, e). AM treatment induced CLDN6 staining at cell–cell borders but the number of CLDN6-positive spots colocalized with ZO-1 was not altered (Fig. 8B, h). However, the size of CLDN6-positive spots (arrows in Fig. 8B,

h) was smaller compared to the control (arrows in Fig. 8A, h). Similarly, the size of occludin-positive spots colocalized with ZO-1 (arrows in Fig. 8A, n) became smaller when treated with AM (arrows in Fig. 8B, n). AM undoubtedly affected the localization of CLDN7. CLDN7-positive spots were not observed even though ZO-1-positive spots were still observed on the surface of 3D cultures (arrowheads in Fig. 8B, j–l). CLDN7 staining at cell–cell borders in deeper layers was significantly decreased (Fig. 8B, k).

## Discussion

K38 cells grown in low calcium medium were seeded onto filters of culture inserts at confluent cell density and induced to form cell–cell junction by addition of calcium before airlifting was performed to induce stratification. However, stratification is not achieved if the cells fail to form cell–cell junctions. Thus, there are two critical steps, cell–cell junction formation (the first step) and stratification (the second step), in the 3D culture system. In the course of stratification, cells differentiate, migrate, and reconstitute cell–cell junctions including TJs. We are interested in whether stress-activated MAPKs affect cell–cell junction formation and stratification. In this study we used 2D and 3D cultures to examine the effect of AM on cell–cell junction formation and stratification, respectively. From the 3D culture experiments, we found that p38 activation removed CLDN7 from the TJs and decreased the TER as well as the change of epithelial morphology; however, the effect of p38 activation was not clarified in 2D experiments. The 2D experiments revealed that JNK activation suppressed the formation and maturation of cell–cell junctions.

### *K38 3D cultures formed non-keratinized stratified epithelium*

In this study, we used K38 3D cultures as a model for non-keratinized stratified epithelium because the 3D cultures expressed K4 but not LOR, in addition to the absence of a cornified

layer. Inconsistent with our result, K38 3D cultures were previously reported to form keratinized stratified epithelium, with expression of K10, filaggrin, and involucrin in the suprabasal cells and formation of a cornified layer (Vollmers et al. 2012). However, the purported cornified layer was too thin to be verified. Although filaggrin (Smith and Dale 1986) and involucrin (Gibbs and Ponec 2000) have also been detected in non-keratinized epithelium such as buccal mucosal epithelium, LOR was restricted to keratinized epithelium (Gibbs and Ponec 2000). K4 was localized in non-keratinized epithelium, such as in the buccal mucosa and esophagus (Dale et al. 1990). Therefore, the present K38 3D cultures reconstituted non-keratinized epithelium but not keratinized epithelium. We investigated the localization of CLDNs 1, 4, and 7 in K38 cells, as they were detected in human non-keratinized epithelium such as buccal and lip epithelia (Lourenco et al. 2010). In addition, we examined CLDN6, an embryonic CLDN (Morita et al. 2002).

***Maturation of cell–cell junctions from zipper-like junctions into string-like junctions was suppressed by AM treatment in K38 2D cultures***

In K38 2D cultures, the zipper-like staining for ZO-1 is probably equivalent to spot-like adherens junctions (AJs) that consist of E-cadherin (Suzuki et al. 2002; Vaezi et al. 2002; Vasioukhin et al. 2000; Yonemura et al. 1995). It was observed in the early stage of cell–cell junction formation induced by calcium at 2 h, gradually replaced with the string-like staining formed by fusion of the zipper-like staining at 6 h, and completely replaced at 12 h. Some zipper-like staining for ZO-1 was negative for CLDN4 in the control (Fig. 2d, g), suggesting that E-cadherin first formed spot-like AJs to where CLDN4 was later recruited. This hypothesis is supported by a previous study, in which CLDN1 was recruited to spot-like AJs later than ZO-1 and occludin (Suzuki et al. 2002). In MDCK cells, ZO-1 was first colocalized with E-cadherin through binding to catenins and later separated from E-cadherin during the

formation of TJs (Rajasekaran et al. 1996). Consistently, ZO-1 was first colocalized with E-cadherin in spot-like AJs and later separated from E-cadherin to form belt-like junctions with occludin at the most apical region of the lateral plasma membrane (Ando-Akatsuka et al. 1999; Pummi et al. 2001). In the present study, AM treatment suppressed the formation of the string-like staining for ZO-1 and incorporation of CLDNs 4, 6, and 7 into cell–cell contacts, suggesting that the activation of JNK and/or p38 may suppress maturation of cell–cell junctions from spot-like junctions into belt-like junctions. Depletion of extracellular calcium disrupts AJs, leading to disruption of TJs, indicating that AJs are required for the formation of TJs. In human primary keratinocytes, JNK inhibited AJ formation by phosphorylation of β-catenin, whereas inhibition of JNK resulted in dephosphorylation of β-catenin, leading to AJ formation (Lee et al. 2009; Lee et al. 2011). In the human colonic epithelial cell lines, SK-CO15 and T84, JNK1 activation by Rho-dependent kinase induced disruption of AJs and TJs (Naydenov et al. 2009). Based on these results, JNK activation by AM may inhibit maturation of AJs from a spot-like to belt-like pattern, and thus suppressing the incorporation of CLDNs 4, 6, and 7 into cell–cell junctions to form TJs.

***Inhibition of JNK restored the formation of string-like junctions in K38 2D cultures by AM treatment***

Activation of p38α/γ by AM plus SP600125 in K38 cells restored the formation of string-like staining for ZO-1 at 12 h, whereas activation of JNK by AM plus BIRB 796 or activation of JNK and p38γ by AM plus SB202190 did not restore this formation. Furthermore, neither JNK nor p38 was activated in the control, which showed string-like-staining for ZO-1 at 12 h. These results indicate that inhibition of JNK was necessary to induce string-like staining for ZO-1 when treated with AM, and that activation of p38α/γ did not inhibit induction. Consistently, activation of JNK triggered by calcium depletion induced the disassembly of

ZO-1 from cell–cell contacts, while inhibition of JNK activation suppressed the disassembly of ZO-1 (Naydenov et al. 2009). However, it is still unknown why CLDNs 4, 6, and 7 did not fully colocalize with the string-like staining for ZO-1 in K38 cells treated with AM plus SP600125. It is possible that SP600125 did not completely inhibit JNK activation, thus inhibiting recruitment of CLDNs to the location of ZO-1, or that activation of p38α/γ inhibited the recruitment of these CLDNs. It was previously reported that activation of p38δ by high calcium induced the expression and accumulation of ZO-1 in cell–cell contacts in human keratinocytes (Siljamaki et al. 2014). However, this is not possible for K38 cells as they did not express p38δ and addition of calcium did not activate p38.

***Long-term activation of p38 in K38 3D cultures removed CLDN7 from TJs and decreased the TER***

Long-term treatment of K38 3D cultures with AM for 2 weeks activated only p38, removed CLDN7 from ZO-1 positive spots in the first and second layers, increased CLDN6, and decreased TER. Although CLDN4 and CLDN6 levels were decreased and increased, respectively, CLDN4 and CLDN6 spots that colocalized with ZO-1 were not altered. CLDN1 was not detected in ZO-1-positive spots, even in the control. These results suggest that marked reduction of CLDN7 from TJs corresponding to the ZO-1-positive spots on the surface of 3D cultures may cause the decrease of TER. Activation of p38 by aspirin consistently reduced CLDN7 levels and decreased TER in a human gastric adenocarcinoma cell line, MKN28 (Oshima et al. 2008). Regulation of CLDN expression by p38 and JNK was also reported in a mouse mammary epithelial cell line (31EG4-2A4), although expression of CLDN7 mRNA was increased by inhibition of JNK2 (Carrozzino et al. 2009). These results indicate that expression of CLDN7 is regulated by p38 and/or JNK in a cell-specific manner. It has been reported that the transcription factors, hepatocyte nuclear factor 4α (HNF4α)

(Farkas et al. 2015) and ELF3 (Kohno et al. 2006), regulate expression of CLDN7 in intestinal epithelial cells and biphasic synovial sarcoma, respectively.

Knockdown of CLDN7 decreased TER in cation-selective MDCK cells, while it increased TER in anion-selective LLC-PK1 cells, suggesting that CLDN7 functions as a paracellular barrier to $Na^+$ in MDCK cells but as a paracellular channels for $Cl^-$ in LLC-PK1 cells (Hou et al. 2006). Controversially, overexpression of CLDN7 in LLC-PK1 cells increased TER by concurrently decreasing the paracellular conductance to $Cl^-$ and increasing the paracellular conductance to $Na^+$ (Alexandre et al. 2005). Knockdown of CLDN7 decreased TER in Caco-2 cells (Farkas et al. 2015). Our result is consistent with these results, except for the knockdown of CLDN7 in LLC-PK1 cells. Because TER is determined by the combination and mixing ratios of CLDN isoforms, we need to examine which CLDN isoforms in addition to 1, 4, 6, and 7 are expressed in K38 cells.

There was a discrepancy in p38 phosphorylation between 2D and 3D cultures after AM treatment. JNK and p38 were transiently activated in 2D cultures, while only p38 was activated in 3D cultures. The discrepancy might be caused by difference in the duration of AM treatment or culture system (2D vs 3D). In the stratified epithelium formed by K38 3D cultures, the degree of differentiationof the keratinocytes varied from the basal to superficial cells, as shown by K4 expression; K4 expression was low in the basal cells but high in suprabasal cells (Fig. 1B, a). Suprabasal cells in 3D cultures might be differentiated, compared to cells in 2D cultures. Thus, a difference in degree of differentiation may cause the discrepancy.

***Plasma membrane localizations of CLDNs 6 and 7 in suprabasal cells increased and decreased, respectively, by the long-term activation of p38 in K38 3D cultures***

CLDNs 4 and 7 were localized at cell–cell borders of the suprabasal cells in K38 3D

cultures, while CLDNs 1 and 6 were localized diffusely in the cytoplasm of suprabasal cells. In the human or mouse epidermis, CLDNs 1, 4, 6, 7, 11, 12, 17, and 18 were localized at cell–cell borders in the granular, spinous, and occasionally basal layers (Brandner et al. 2002; Brandner et al. 2006; Brandner et al. 2003; Furuse et al. 2002; Haftek et al. 2011; Igawa et al. 2011; Morita et al. 2004; Troy et al. 2005). These results indicate that CLDNs are localized to the entire plasma membranes of epidermal keratinocytes in the basal and spinous layers where TJs are not formed, in addition to cells in the granular layer where TJs are formed (Furuse et al. 2002; Kubo et al. 2009; Tsuruta et al. 2002). Similarly, in the cells of simple epithelium, some CLDN isoforms are localized along the entire lateral plasma membrane (Coyne et al. 2003; Fujita et al. 2006; Guan et al. 2005; Inai et al. 2005; Inai et al. 2007; Li et al. 2004; Rahner et al. 2001) where TJs are not formed. The biological roles of these ectopic CLDNs in the simple epithelium and the epidermis have not yet been established. We speculate that CLDNs in plasma membrane in the spinous layer may form TJs when the spinous cells reach the granular layer during their migration from the basal to cornified layer. Thus, formation of TJs by CLDNs in the plasma membrane is regulated not to form TJs until keratinocytes reach the granular layer. Plasma membrane localizations of CLDNs 4, 6, and 7 in suprabasal cells were steady, increased, and decreased, respectively, by long-term activation of p38 in K38 3D cultures. This result suggests that p38 is involved in regulating the plasma membrane localization of CLDNs depending on the CLDN isoforms.

**Acknowledgements**

This work was supported in part by a Grant-in-Aid for Scientific Research (C) (No. 26460285) from the Ministry of Education, Culture, Sports, Science, and Technology in Japan.

## Conflict of Interest

The authors declare that they have no conflict of interest.

## References


Al Yassin TM, Toner PG (1977) Fine structure of squamous epitheilum and submucosal glands of human oesophagus. J Anat 123:705-721

Alexandre MD, Lu Q, Chen YH (2005) Overexpression of claudin-7 decreases the paracellular Cl- conductance and increases the paracellular Na+ conductance in LLC-PK1 cells. J Cell Sci 118:2683-2693. https://doi.org/10.1242/jcs.02406

Ando-Akatsuka Y, Yonemura S, Itoh M, Furuse M, Tsukita S (1999) Differential behavior of E-cadherin and occludin in their colocalization with ZO-1 during the establishment of epithelial cell polarity. J Cell Physiol 179:115-125. https://doi.org/10.1002/(SICI)1097-4652(199905)179:2<115::AID-JCP1>3.0.CO;2-T

Aono S, Hirai Y (2008) Phosphorylation of claudin-4 is required for tight junction formation in a human keratinocyte cell line. Exp Cell Res 314:3326-3339. https://doi.org/10.1016/j.yexcr.2008.08.012

Babkair H, Yamazaki M, Uddin MS, Maruyama S, Abe T, Essa A, Sumita Y, Ahsan MS, Swelam W, Cheng J, Saku T (2016) Aberrant expression of the tight junction molecules claudin-1 and zonula occludens-1 mediates cell growth and invasion in oral squamous cell carcinoma. Hum Pathol 57:51-60. https://doi.org/10.1016/j.humpath.2016.07.001

Ban Y, Dota A, Cooper LJ, Fullwood NJ, Nakamura T, Tsuzuki M, Mochida C, Kinoshita S (2003) Tight junction-related protein expression and distribution in human corneal epithelium. Exp Eye Res 76:663-669

Barrett AW, Selvarajah S, Franey S, Wills KA, Berkovitz BK (1998) Interspecies variations in

oral epithelial cytokeratin expression. J Anat 193 (Pt 2):185-193

Bogoyevitch MA, Court NW (2004) Counting on mitogen-activated protein kinases--ERKs 3, 4, 5, 6, 7 and 8. Cell Signal 16:1345-1354 doi:10.1016/j.cellsig.2004.05.004

Brandner JM, Kief S, Grund C, Rendl M, Houdek P, Kuhn C, Tschachler E, Frankee WW, Moll I (2002) Organization and formation of the tight junction system in human epidermis and cultured keratinocytes. Eur J Cell Biol 81:253-263. https://doi.org/10.1078/0171-9335-00244

Brandner JM, Kief S, Wladykowski E, Houdek P, Moll I (2006) Tight junction proteins in the skin. Skin Pharmacol Physiol 19:71-77. https://doi.org/10.1159/000091973

Brandner JM, McIntyre M, Kief S, Wladykowski E, Moll I (2003) Expression and localization of tight junction-associated proteins in human hair follicles. Arch Dermatol Res 295:211-221. https://doi.org/10.1007/s00403-003-0418-3

Carrozzino F, Pugnale P, Feraille E, Montesano R (2009) Inhibition of basal p38 or JNK activity enhances epithelial barrier function through differential modulation of claudin expression. Am J Physiol Cell Physiol 297:C775-787. https://doi.org/10.1152/ajpcell.00084.2009

Coyne CB, Gambling TM, Boucher RC, Carson JL, Johnson LG (2003) Role of claudin interactions in airway tight junctional permeability. Am J Physiol Lung Cell Mol Physiol 285:L1166-1178. https://doi.org/10.1152/ajplung.00182.2003

Dale BA, Salonen J, Jones AH (1990) New approaches and concepts in the study of differentiation of oral epithelia. Crit Rev Oral Biol Med 1:167-190

Davis RJ (2000) Signal transduction by the JNK group of MAP kinases. Cell 103:239-252

Dongari-Bagtzoglou A, Kashleva H (2006) Development of a highly reproducible three-dimensional organotypic model of the oral mucosa. Nat Protoc 1:2012-2018. https://doi.org/10.1038/nprot.2006.323

Farkas AE, Hilgarth RS, Capaldo CT, Gerner-Smidt C, Powell DR, Vertino PM, Koval M, Parkos CA, Nusrat A (2015) HNF4alpha regulates claudin-7 protein expression during intestinal epithelial differentiation. Am J Pathol 185:2206-2218. https://doi.org/10.1016/j.ajpath.2015.04.023

Frankart A, Malaisse J, De Vuyst E, Minner F, de Rouvroit CL, Poumay Y (2012) Epidermal morphogenesis during progressive in vitro 3D reconstruction at the air-liquid interface. Exp Dermatol 21:871-875. https://doi.org/10.1111/exd.12020

Fujita H, Chiba H, Yokozaki H, Sakai N, Sugimoto K, Wada T, Kojima T, Yamashita T, Sawada N (2006) Differential expression and subcellular localization of claudin-7, -8, -12, -13, and -15 along the mouse intestine. J Histochem Cytochem 54:933-944. https://doi.org/10.1369/jhc.6A6944.2006

Furuse M, Hata M, Furuse K, Yoshida Y, Haratake A, Sugitani Y, Noda T, Kubo A, Tsukita S (2002) Claudin-based tight junctions are crucial for the mammalian epidermal barrier: a lesson from claudin-1-deficient mice. J Cell Biol 156:1099-1111. https://doi.org/10.1083/jcb.200110122

Furuse M, Sasaki H, Fujimoto K, Tsukita S (1998) A single gene product, claudin-1 or -2, reconstitutes tight junction strands and recruits occludin in fibroblasts. J Cell Biol 143:391-401

Gibbs S, Ponec M (2000) Intrinsic regulation of differentiation markers in human epidermis, hard palate and buccal mucosa. Arch Oral Biol 45:149-158

Guan X, Inai T, Shibata Y (2005) Segment-specific expression of tight junction proteins, claudin-2 and -10, in the rat epididymal epithelium. Arch Histol Cytol 68:213-225

Haftek M, Callejon S, Sandjeu Y, Padois K, Falson F, Pirot F, Portes P, Demarne F, Jannin V (2011) Compartmentalization of the human stratum corneum by persistent tight junction-like structures. Exp Dermatol 20:617-621. https://doi.org/10.1111/j.1600-

0625.2011.01315.x

Hagemann C, Blank JL (2001) The ups and downs of MEK kinase interactions. Cell Signal 13:863-875

Hou J, Gomes AS, Paul DL, Goodenough DA (2006) Study of claudin function by RNA interference. J Biol Chem 281:36117-36123. https://doi.org/10.1074/jbc.M608853200

Igawa S, Kishibe M, Murakami M, Honma M, Takahashi H, Iizuka H, Ishida-Yamamoto A (2011) Tight junctions in the stratum corneum explain spatial differences in corneodesmosome degradation. Exp Dermatol 20:53-57. https://doi.org/10.1111/j.1600-0625.2010.01170.x

Inai T, Sengoku A, Guan X, Hirose E, Iida H, Shibata Y (2005) Heterogeneity in expression and subcellular localization of tight junction proteins, claudin-10 and -15, examined by RT-PCR and immunofluorescence microscopy. Arch Histol Cytol 68:349-360.

Inai T, Sengoku A, Hirose E, Iida H, Shibata Y (2007) Claudin-7 expressed on lateral membrane of rat epididymal epithelium does not form aberrant tight junction strands. Anat Rec (Hoboken) 290:1431-1438. https://doi.org/10.1002/ar.20597

Inai T, Sengoku A, Hirose E, Iida H, Shibata Y (2008) Comparative characterization of mouse rectum CMT93-I and -II cells by expression of claudin isoforms and tight junction morphology and function. Histochem Cell Biol 129:223-232.

Jones KB, Klein OD (2013) Oral epithelial stem cells in tissue maintenance and disease: the first steps in a long journey. Int J Oral Sci 5:121-129. https://doi.org/10.1038/ijos.2013.46

Kalabis J, Wong GS, Vega ME, Natsuizaka M, Robertson ES, Herlyn M, Nakagawa H, Rustgi AK (2012) Isolation and characterization of mouse and human esophageal epithelial cells in 3D organotypic culture. Nat Protoc 7:235-246. https://doi.org/10.1038/nprot.2011.437

Kim HJ, Tinling SP, Chole RA (2002) Expression patterns of cytokeratins in cholesteatomas: evidence of increased migration and proliferation. J Korean Med Sci 17:381-388

Kitagawa N, Inai Y, Higuchi Y, Iida H, Inai T (2014) Inhibition of JNK in HaCaT cells induced tight junction formation with decreased expression of cytokeratin 5, cytokeratin 17 and desmoglein 3. Histochem Cell Biol 142:389-399. https://doi.org/10.1007/s00418-014-1219-9

Kohno Y, Okamoto T, Ishibe T, Nagayama S, Shima Y, Nishijo K, Shibata KR, Fukiage K, Otsuka S, Uejima D, Araki N, Naka N, Nakashima Y, Aoyama T, Nakayama T, Nakamura T, Toguchida J (2006) Expression of claudin7 is tightly associated with epithelial structures in synovial sarcomas and regulated by an Ets family transcription factor, ELF3. J Biol Chem 281:38941-38950. https://doi.org/10.1074/jbc.M608389200

Kojima T, Fuchimoto J, Yamaguchi H, Ito T, Takasawa A, Ninomiya T, Kikuchi S, Ogasawara N, Ohkuni T, Masaki T, Hirata K, Himi K, Sawada N (2010) c-Jun N-terminal kinase is largely involved in the regulation of tricellular tight junctions via tricellulin in human pancreatic duct epithelial cells. J Cell Physiol 225:720-733. https://doi.org/10.1002/jcp.22273

Kubo A, Nagao K, Yokouchi M, Sasaki H, Amagai M (2009) External antigen uptake by Langerhans cells with reorganization of epidermal tight junction barriers. J Exp Med 206:2937-2946. https://doi.org/10.1084/jem.20091527

Kyriakis JM, Avruch J (2001) Mammalian mitogen-activated protein kinase signal transduction pathways activated by stress and inflammation. Physiol Rev 81:807-869

Lee MH, Koria P, Qu J, Andreadis ST (2009) JNK phosphorylates beta-catenin and regulates adherens junctions. FASEB J 23:3874-3883. https://doi.org/10.1096/fj.08-117804

Lee MH, Padmashali R, Koria P, Andreadis ST (2011) JNK regulates binding of alpha-catenin to adherens junctions and cell-cell adhesion. FASEB J 25:613-623.

https://doi.org/10.1096/fj.10-161380

Li WY, Huey CL, Yu AS (2004) Expression of claudin-7 and -8 along the mouse nephron. Am J Physiol Renal Physiol 286:F1063-1071. https://doi.org/10.1152/ajprenal.00384.2003

Lichti U, Anders J, Yuspa SH (2008) Isolation and short-term culture of primary keratinocytes, hair follicle populations and dermal cells from newborn mice and keratinocytes from adult mice for in vitro analysis and for grafting to immunodeficient mice. Nat Protoc 3:799-810. https://doi.org/10.1038/nprot.2008.50

Lourenco SV, Coutinho-Camillo CM, Buim ME, Pereira CM, Carvalho AL, Kowalski LP, Soares FA (2010) Oral squamous cell carcinoma: status of tight junction claudins in the different histopathological patterns and relationship with clinical parameters. A tissue-microarray-based study of 136 cases. J Clin Pathol 63:609-614. https://doi.org/10.1136/jcp.2009.070409

Minakami M, Kitagawa N, Iida H, Anan H, Inai T (2015) p38 Mitogen-activated protein kinase and c-Jun NH2-terminal protein kinase regulate the accumulation of a tight junction protein, ZO-1, in cell-cell contacts in HaCaT cells. Tissue Cell 47:1-9. https://doi.org/10.1016/j.tice.2014.10.001

Moll R, Divo M, Langbein L (2008) The human keratins: biology and pathology. Histochem Cell Biol 129:705-733. https://doi.org/10.1007/s00418-008-0435-6

Morita K, Furuse M, Yoshida Y, Itoh M, Sasaki H, Tsukita S, Miyachi Y (2002) Molecular architecture of tight junctions of periderm differs from that of the maculae occludentes of epidermis. J Invest Dermatol 118:1073-1079. https://doi.org/10.1046/j.1523-1747.2002.01774.x

Morita K, Tsukita S, Miyachi Y (2004) Tight junction-associated proteins (occludin, ZO-1, claudin-1, claudin-4) in squamous cell carcinoma and Bowen's disease. Br J Dermatol 151:328-334. https://doi.org/10.1111/j.1365-2133.2004.06029.x

Nakatsukasa M, Kawasaki S, Yamasaki K, Fukuoka H, Matsuda A, Tsujikawa M, Tanioka H, Nagata-Takaoka M, Hamuro J, Kinoshita S (2010) Tumor-associated calcium signal transducer 2 is required for the proper subcellular localization of claudin 1 and 7: implications in the pathogenesis of gelatinous drop-like corneal dystrophy. Am J Pathol 177:1344-1355. https://doi.org/10.2353/ajpath.2010.100149

Naydenov NG, Hopkins AM, Ivanov AI (2009) c-Jun N-terminal kinase mediates disassembly of apical junctions in model intestinal epithelia. Cell Cycle 8:2110-2121. https://doi.org/10.4161/cc.8.13.8928

Oshima T, Gedda K, Koseki J, Chen X, Husmark J, Watari J, Miwa H, Pierrou S (2011) Establishment of esophageal-like non-keratinized stratified epithelium using normal human bronchial epithelial cells. Am J Physiol Cell Physiol 300:C1422-1429. https://doi.org/10.1152/ajpcell.00376.2010

Oshima T, Koseki J, Chen X, Matsumoto T, Miwa H (2012) Acid modulates the squamous epithelial barrier function by modulating the localization of claudins in the superficial layers. Lab Invest 92:22-31. https://doi.org/10.1038/labinvest.2011.139

Oshima T, Miwa H, Joh T (2008) Aspirin induces gastric epithelial barrier dysfunction by activating p38 MAPK via claudin-7. Am J Physiol Cell Physiol 295:C800-806. https://doi.org/10.1152/ajpcell.00157.2008

Pearson LL, Castle BE, Kehry MR (2001) CD40-mediated signaling in monocytic cells: up-regulation of tumor necrosis factor receptor-associated factor mRNAs and activation of mitogen-activated protein kinase signaling pathways. Int Immunol 13:273-283

Poumay Y, Dupont F, Marcoux S, Leclercq-Smekens M, Herin M, Coquette A (2004) A simple reconstructed human epidermis: preparation of the culture model and utilization in in vitro studies. Arch Dermatol Res 296:203-211. https://doi.org/10.1007/s00403-004-0507-y

Pummi K, Malminen M, Aho H, Karvonen SL, Peltonen J, Peltonen S (2001) Epidermal tight junctions: ZO-1 and occludin are expressed in mature, developing, and affected skin and in vitro differentiating keratinocytes. J Invest Dermatol 117:1050-1058. https://doi.org/10.1046/j.0022-202x.2001.01493.x

Rahner C, Mitic LL, Anderson JM (2001) Heterogeneity in expression and subcellular localization of claudins 2, 3, 4, and 5 in the rat liver, pancreas, and gut. Gastroenterology 120:411-422

Rajasekaran AK, Hojo M, Huima T, Rodriguez-Boulan E (1996) Catenins and zonula occludens-1 form a complex during early stages in the assembly of tight junctions. J Cell Biol 132:451-463

Reichelt J, Haase I (2010) Establishment of spontaneously immortalized keratinocyte lines from wild-type and mutant mice. Methods Mol Biol 585:59-69. https://doi.org/10.1007/978-1-60761-380-0_5

Schaeffer HJ, Weber MJ (1999) Mitogen-activated protein kinases: specific messages from ubiquitous messengers. Mol Cell Biol 19:2435-2444

Segrelles C, Holguin A, Hernandez P, Ariza JM, Paramio JM, Lorz C (2011) Establishment of a murine epidermal cell line suitable for in vitro and in vivo skin modelling. BMC Dermatol 11:9. https://doi.org/10.1186/1471-5945-11-9

Seo A, Kitagawa N, Matsuura T, Sato H, Inai T (2016) Formation of keratinocyte multilayers on filters under airlifted or submerged culture conditions in medium containing calcium, ascorbic acid, and keratinocyte growth factor. Histochem Cell Biol 146:585-597. https://doi.org/10.1007/s00418-016-1472-1

Siljamaki E, Raiko L, Toriseva M, Nissinen L, Nareoja T, Peltonen J, Kahari VM, Peltonen S (2014) p38delta mitogen-activated protein kinase regulates the expression of tight junction protein ZO-1 in differentiating human epidermal keratinocytes. Arch

Dermatol Res 306:131-141. https://doi.org/10.1007/s00403-013-1391-0

Smith SA, Dale BA (1986) Immunologic localization of filaggrin in human oral epithelia and correlation with keratinization. J Invest Dermatol 86:168-172

Suzuki A, Ishiyama C, Hashiba K, Shimizu M, Ebnet K, Ohno S (2002) aPKC kinase activity is required for the asymmetric differentiation of the premature junctional complex during epithelial cell polarization. J Cell Sci 115:3565-3573

Takaoka M, Nakamura T, Ban Y, Kinoshita S (2007) Phenotypic investigation of cell junction-related proteins in gelatinous drop-like corneal dystrophy. Invest Ophthalmol Vis Sci 48:1095-1101. https://doi.org/10.1167/iovs.06-0740

Torma H (2011) Regulation of keratin expression by retinoids. Dermatoendocrinol 3:136-140. https://doi.org/10.4161/derm.3.3.15026

Troy TC, Rahbar R, Arabzadeh A, Cheung RM, Turksen K (2005) Delayed epidermal permeability barrier formation and hair follicle aberrations in Inv-Cldn6 mice. Mech Dev 122:805-819. https://doi.org/10.1016/j.mod.2005.03.001

Tsuruta D, Green KJ, Getsios S, Jones JC (2002) The barrier function of skin: how to keep a tight lid on water loss. Trends Cell Biol 12:355-357

Vaezi A, Bauer C, Vasioukhin V, Fuchs E (2002) Actin cable dynamics and Rho/Rock orchestrate a polarized cytoskeletal architecture in the early steps of assembling a stratified epithelium. Dev Cell 3:367-381

Vasioukhin V, Bauer C, Yin M, Fuchs E (2000) Directed actin polymerization is the driving force for epithelial cell-cell adhesion. Cell 100:209-219

Vollmers A, Wallace L, Fullard N, Hoher T, Alexander MD, Reichelt J (2012) Two- and three-dimensional culture of keratinocyte stem and precursor cells derived from primary murine epidermal cultures. Stem Cell Rev 8:402-413. https://doi.org/10.1007/s12015-011-9314-y

Yonemura S, Itoh M, Nagafuchi A, Tsukita S (1995) Cell-to-cell adherens junction formation and actin filament organization: similarities and differences between non-polarized fibroblasts and polarized epithelial cells. J Cell Sci 108 (Pt 1):127-142

Yoshida Y, Ban Y, Kinoshita S (2009) Tight junction transmembrane protein claudin subtype expression and distribution in human corneal and conjunctival epithelium. Invest Ophthalmol Vis Sci 50:2103-2108. https://doi.org/10.1167/iovs.08-3046

**Figure legends**

**Fig. 1** 3D cultures of K38 and COCA cells formed non-keratinized and keratinized stratified squamous epithelium-like structures, respectively. (A) K38 (a–c) and COCA (d–f) cells seeded on the filters of cell culture inserts were airlifted for 1 (a, d), 2 (b, e), or 3 (c, f) weeks. Cryosections were stained with HE. The cornified layer stained pink with eosin was observed in COCA 3D cultures but not K38. Scale bar: 20 μm. (B) Cryosections obtained from 3D cultures of K38 (a) and COCA (b) cells for 2 weeks were double stained with antibodies against K4 (green) and LOR (red). K4 or LOR was detected in K38 or COCA 3D cultures, respectively. Nuclei were stained with DAPI (blue). Scale bar: 20 μm. (C) 2D cultures of HEKa, COCA, and K38 cells in the presence of 1.2 mM calcium were lysed, fractionated by SDS-PAGE, and transferred onto PVDF membranes. Immunoblotting was performed using antibodies against ERK, JNK1, JNK2, p38α, p38β, p38γ, p38δ, CLDNs 1, 4, 6, and 7, and β-actin. After primary and secondary antibodies were stripped from the blots, the membranes were reprobed. Observed band sizes were as follows: ERK, 42 (lower band) and 44 (upper band) kDa; JNK1 and JNK2, 46 (lower band) and 54 (upper band) kDa; p38α, 40 kDa; p38β, 43 kDa; p38γ, 46 kDa; p38δ, 43 kDa; CLDNs 1, 4, 6, and 7, ~20 kDa; β-actin, 42 kDa.

**Fig. 2** Effect of AM on the localization of CLDN4 and ZO-1 in K38 2D culture after the

induction of cell–cell junctions by calcium for 12 h. K38 cells cultured in low calcium FAD medium on glass slides were treated with 1.2 mM calcium and either 0.2% DMSO (d–l) or 100 nM AM (m–u) for 2 h (d–f, m–o), 6 h (g–i, p–r), and 12 h (j–l, s–u). Cells before treatment are shown in a–c. Cells were double stained with antibodies against CLDN4 (a, d, g, j, m, p, s, green) and ZO-1 (b, e, h, k, n, q, t, red). Merged images are shown in c, f, i, l, o, r, and u. Nuclei were stained with DAPI (blue). Arrows indicate string-like staining positive for both CLDN4 and ZO-1 while arrowheads indicate zipper-like staining positive for ZO-1 but not for CLDN4. String-like staining positive for CLDN4 and ZO-1 was established at 12 h but was inhibited in the presence of AM. Scale bar: 20 μm.

**Fig. 3** Short-term effect of AM and AM plus an inhibitor for p38 or JNK on the phosphorylation of MAPKs in K38 2D cultures. Confluent K38 cells treated with 1.2 mM calcium plus 0.2% DMSO (vehicle), AM (100 nM), AM plus 20 μM SB202190, AM plus 20 μM BIRB 796, or AM plus 20 μM SP600125 for 0.5 or 12 h. Cells were lysed, fractionated by SDS-PAGE, and transferred onto PVDF membranes. Immunoblotting was performed using antibodies against P-ERK, ERK, P-p38, p38, P-JNK, JNK, and β-actin. Membranes were reprobed after stripping primary and secondary antibodies. AM transiently phosphorylated both JNK and p38 at 0.5 h whereas phosphorylated JNK and p38 almost disappeared by 12 h. Phosphorylation of JNK or p38 was inhibited by SP600125 or BIRB 796, respectively, while that of p38 was not inhibited by SB202190. The observed band sizes were as follows: P-ERK and ERK, 42 (lower band) and 44 (upper band) kDa; P-JNK and JNK, 46 (lower band) and 54 (upper band) kDa; P-p38 and p38, 43 kDa; β-actin, 42 kDa.

**Fig. 4** Short-term effect of AM and AM plus an inhibitor for p38 or JNK on localization of ZO-1 and CLDN4 in K38 2D cultures. Confluent K38 cells treated with 1.2 mM calcium plus

0.2% DMSO (vehicle), AM (100 nM), AM plus 20 μM SB202190, AM plus 20 μM BIRB 796, or AM plus 20 μM SP600125 for 12 h. Cells were double stained with antibodies against ZO-1 (a, d, g, j, m, green) and CLDN4 (b, e, h, k, n, red). Merged images are shown in c, f, i, l, and o. Nuclei were stained with DAPI (blue). Arrows indicate string-like staining positive for both ZO-1 and CLDN4 while small arrowheads indicate zipper-like staining positive for ZO-1 but not CLDN4. String-like staining for ZO-1 was restored by AM plus SP600125 and most, but not all, string-like staining was positive for CLDN4. Large arrowheads in m–o indicate string-like staining positive for ZO-1 but not for CLDN4. Scale bar: 20 μm.

**Fig. 5** Short-term effect of AM and AM plus an inhibitor for p38 or JNK on localization of ZO-1 and CLDN6 in K38 2D cultures. Confluent K38 cells treated with 1.2 mM calcium plus 0.2% DMSO (vehicle), AM (100 nM), AM plus 20 μM SB202190, AM plus 20 μM BIRB 796, or AM plus 20 μM SP600125 for 12 h. Cells were double stained with antibodies against ZO-1 (a, d, g, j, m, green) and CLDN6 (b, e, h, k, n, red). Merged images are shown in c, f, i, l, and o. Nuclei were stained with DAPI (blue). Arrows indicate string-like staining positive for ZO-1 and CLDN6, while small arrowheads indicate zipper-like staining positive for ZO-1 but not CLDN6. AM treatment decreased staining intensity for CLDN6, which was not restored by SB202190 or BIRB 796. String-like staining for ZO-1 was restored by AM plus SP600125, but CLDN6 staining was not restored as compared to the control. Large arrowheads in m–o indicate string-like staining positive for ZO-1 but not for CLDN6. Scale bar: 20 μm.

**Fig. 6** Short-term effect of AM and AM plus an inhibitor for p38 or JNK on localization of ZO-1 and CLDN7 in K38 2D cultures. Confluent K38 cells treated with 1.2 mM calcium plus 0.2% DMSO (vehicle), AM (100 nM), AM plus 20 μM SB202190, AM plus 20 μM BIRB

796, or AM plus 20 μM SP600125 for 12 h. Cells were double stained with antibodies against ZO-1 (a, d, g, j, m, green) and CLDN7 (b, e, h, k, n, red). Merged images are shown in c, f, i, l, and o. Nuclei were stained with DAPI (blue). Arrows indicate string-like staining positive for both ZO-1 and CLDN7 while small arrowheads indicate zipper-like staining positive for ZO-1 but not for CLDN7. Staining intensity for CLDN7 was not significantly decreased by AM. String-like staining for ZO-1 was restored by AM plus SP600125, but CLDN7 was not fully restored, although CLDN7 was detected in the lateral plasma membrane as observed in the control. Large arrowheads in m–o indicate string-like staining positive for ZO-1 but not for CLDN7. Scale bar: 20 μm.

**Fig. 7** Long-term effects of AM on morphology, TER, and protein expression of MAPKs, E-cadherin, and TJ proteins in K38 3D cultures. (A) K38 cells seeded on insert filters were airlifted for 2 weeks in the presence of 0 (a), 30 (b), or 50 (c) nM AM. Cryosections were stained with HE. Scale bar: 20 μm. Flattened cells were observed on the surface of 3D cultures without AM, while hyperplastic cells were detected on the surface in the presence of AM. (B) K38 cells seeded on insert filters were airlifted for 2 weeks in the absence (a) or presence of 50 (b) nM AM. Cryosections were immunostained with anti-E-cadherin antibody (red) to indicate cell boundaries. Nuclei were stained with DAPI (blue). Arrowheads indicate surface cells that were flattened (a) or hyperplastic (b). Scale bar: 20 μm. (C) The TER of K38 3D culture in the presence of 0, 30, or 50 nM AM for 2 weeks was measured. AM was added at the start of airlift and added at each medium change. TER was reduced by ~ 30% by 50 nM AM but not by 30 nM AM. Data represent the mean ± SEM of 2 independent experiments performed in triplicate. $*P < 0.05$ vs control. (D) K38 cells seeded on insert filters were airlifted for 2 weeks in the presence of 0, 30, or 50 nM AM. Cells were lysed, fractionated by SDS-PAGE, and transferred onto PVDF membranes. Immunoblotting was performed using

antibodies against P-JNK, JNK, P-p38, p38, P-ERK, ERK, CLDNs 1, 4, 6, and 7, ZO-1, E-cadherin, and β-actin. Membranes were reprobed after stripping primary and secondary antibodies. Phosphorylation was detected for p38, but not JNK and ERK, when treated with 50 nM AM. Treatment with 50 nM AM increased CLDN1 and remarkably CLDN6, while it decreased CLDN4, ZO-1, E-cadherin, and CLDN7. The observed band sizes were as follows: JNK, 46 (lower band) and 54 (upper band) kDa; P-p38 and p38, 43 kDa; ERK, 42 (lower band) and 44 (upper band) kDa; CLDNs 1, 4, 6, and 7, ~20 kDa; ZO-1, ~225 kDa; E-cadherin, ~135 kDa; β-actin, 42 kDa.

**Fig. 8** Long-term effect of AM on localization of TJ proteins and occludin in K38 3D culture. K38 cells seeded on insert filters were airlifted for 2 weeks in the presence of 0.2% DMSO (A) or 50 nM AM (B). Cryosections were double stained with antibodies against ZO-1 (a, d, g, j, and m) and either CLDNs 1 (b), 4 (e), 6 (h), or 7 (k), or occludin (n). Mouse anti-ZO-1 antibody was used in a, g, and j while rabbit anti-ZO-1 antibody was used in d and m. Merged images are shown in c, f, i, l, and o. Nuclei were stained with DAPI (blue). Arrows indicate staining positive for green and red while arrowheads indicate staining positive for green but not for red. Scale bar: 20 μm. (A) In control, ZO-1-positive spots on the surface of 3D cultures colocalized with CLDNs 4, 6, and 7 but were negative for CLDN1. There were fewer CLDN6-positive spots than ZO-1 positive spots. ZO-1, CLDN4, and CLDN7 were detected at cell–cell contacts in the deeper layers. (B) When treated with AM, ZO-1-positive spots became negative for CLDN7. Furthermore, occludin-positive spots became smaller than those in the control, and CLDN6 was detected at cell–cell contacts in the deeper layers. The number of spots positive for CLDN4 or CLDN6 was not altered.

**Supplementary Fig. 1** Antibody specifications examined by immnoblotting. Cells were

lysed, fractionated by SDS-PAGE, and transferred onto PVDF membranes. Immunoblotting was performed using antibodies against CLDNs 1, 4, 6, and 7, β-actin (A); E-cadherin, rabbit ZO-1, mouse ZO-1, K4 (B); p38, P-p38, ERK, P-ERK, JNK, P-JNK (C); JNK1, JNK2, p38α, p38β, p38γ, and p38δ (D). Membranes were reprobed after stripping primary and secondary antibodies. Membranes were cut along the lines in D. Cell lysates used were as follows: M, MDCK II cells; K, K38; C93, CMT93-II cells; C3D, COCA 3D cultures for 2 week; K3D, K38 3D cultures for 2 week; M', MDCK II cells treated with 1 μM AM for 30 min; M', K38 cells treated with 0.1 μM AM for 30 min; H, HEKa cells; C, COCA. Observed band sizes (arrowheads) were as follows: CLDNs 1, 4, 6, and 7, ~20 kDa; β-actin, 42 kDa; E-cadherin, ~135 kDa; ZO-1 (rabbit) and ZO-1 (mouse), ~225 kDa; K4, 57 kDa; p38 and P-p38, 43 kDa; ERK and P-ERK, 42 (lower band) and 44 (upper band) kDa; JNK, P-JNK, JNK1, and JNK2, 46 (lower band) and 54 (upper band) kDa; p38α, 40 kDa; p38β, 43 kDa; p38γ, 46 kDa; and p38δ, 43 kDa.

**Supplementary Fig. 2** Antibody specifications examined by immunofluorescence localization in MDCK II cells and CMT93-II cells. Cells were double stained with mouse anti-ZO-1 and either rabbit anti-CLDN1 (d–f), anti-CLDN7 (g–i), anti-E-cadherin (j–l), or anti-CLDN6 (v–x) antibodies or rabbit anti-ZO-1 and either mouse anti- CLDN4 (m–o) or anti- occludin (p–r) antibodies. MDCK II cells (a–r) expressing occludin, E-cadherin, and CLDNs 1, 2, 3, 4, and 7and CMT 93-II cells (s–x) expressing occludin, E-cadherin, and CLDNs 2, 4, 6, and 7 were used. In control (a–c, s–u), BSA-PBS was used in place of primary antibodies. Green images (d, g, j, m, p, v) show localization of ZO-1. Red images show localization of CLDN1 (e), CLDN7 (h), E-cadherin (k), CLDN4 (n), occludin (q), and CLDN6 (w). Merged images are shown in c, f, i, l, o, r, u, and x. Nuclei were stained with DAPI (blue). ZO-1 is localized at apical junctions with occludin and CLDNs 1, 4, 6, and 7,

but E-cadherin is localized in lateral cell membrane below apical junctions. Scale bar: 20 μm.

**Supplementary Fig. 3** Controls for immunofluorescence in 2D and 3D cultures. K38 cells seeded on insert filters were airlifted for 2 weeks in the presence of 0.2% DMSO (a–c) or 50 nM AM (d–f). COCA cells seeded on insert filters were airlifted for 2 weeks (g–i). K38 cells (2D cultures) were cultured for 12 h in the presence of 1.2 mM calcium (j–l). Cryosections or 2D cultured cells were incubated with BSA-PBS in place of primary antibodies and then secondary antibodies (a mixture of anti-mouse and anti-rabbit Ig conjugated with either Alexa 488 or Alexa 568). Images derived from Alexa 488 (green) are shown in a, d, g, and j. Images derived from Alexa 568 (red) are shown in b, e, h, and k. Nuclei were stained with DAPI (blue). Merged images are shown in c, f, i, and l. No specific signals were observed in these controls. Scale bar in i is applied to a–i: 20 μm. Scale bar in l is applied to j–l: 20 μm.

**Supplementary Fig. 4** Effect of AM on localization of TJ proteins and E-cadherin in K38 2D culture after induction of cell–cell junctions by calcium for 24 h. K38 cells cultured in low calcium FAD medium on glass slides were treated with 1.2 mM calcium and either 0.2% DMSO (A) or 100 nM AM (B) for 24 h. Cells were double stained with antibodies against ZO-1 (a, d, g, j, m, green) and CLDNs 1 (b, red), 4 (e, red), 6 (h, red), or 7 (k, red), or E-cadherin (n, red). Mouse anti-ZO-1 antibody was used in a, g, j, and m while rabbit anti-ZO-1 antibody was used in d. Merged images are shown in c, f, i, l, and o. Nuclei were stained with DAPI (blue). Arrows indicate string-like staining positive for green and red while arrowheads indicate zipper-like staining positive for green but not for red. Scale bars: 20 μm.

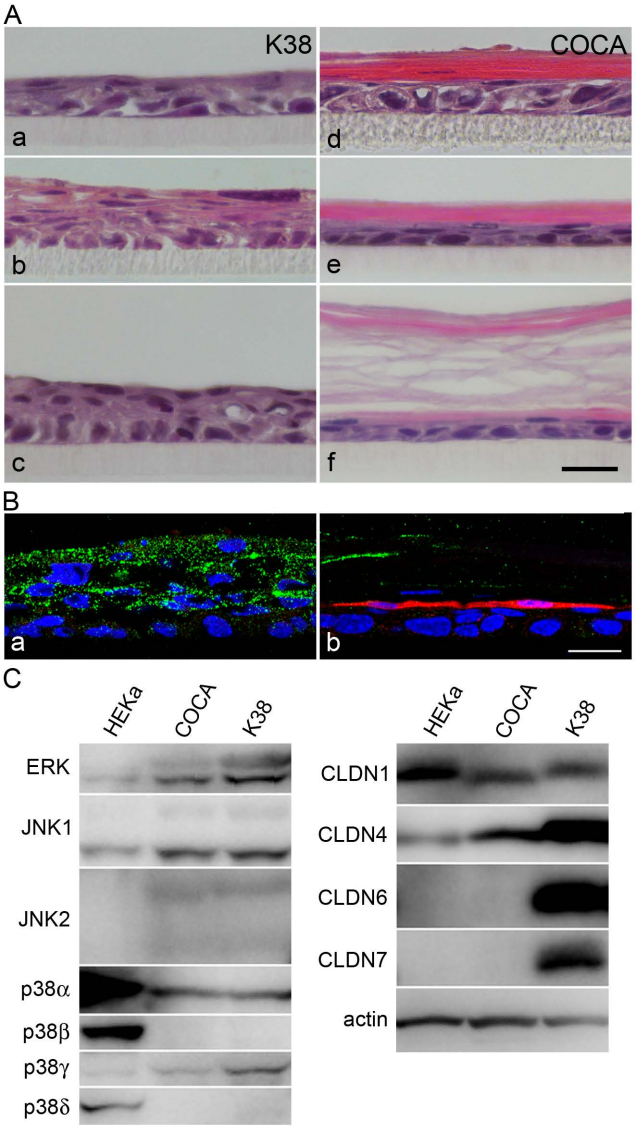
A
K38
COCA
a
b
c
d
e
f
B
a
b
C
HEKa
COCA
K38
ERK
JNK1
JNK2
p38α
p38β
p38γ
p38δ
HEKa
COCA
K38
CLDN1
CLDN4
CLDN6
CLDN7
actin

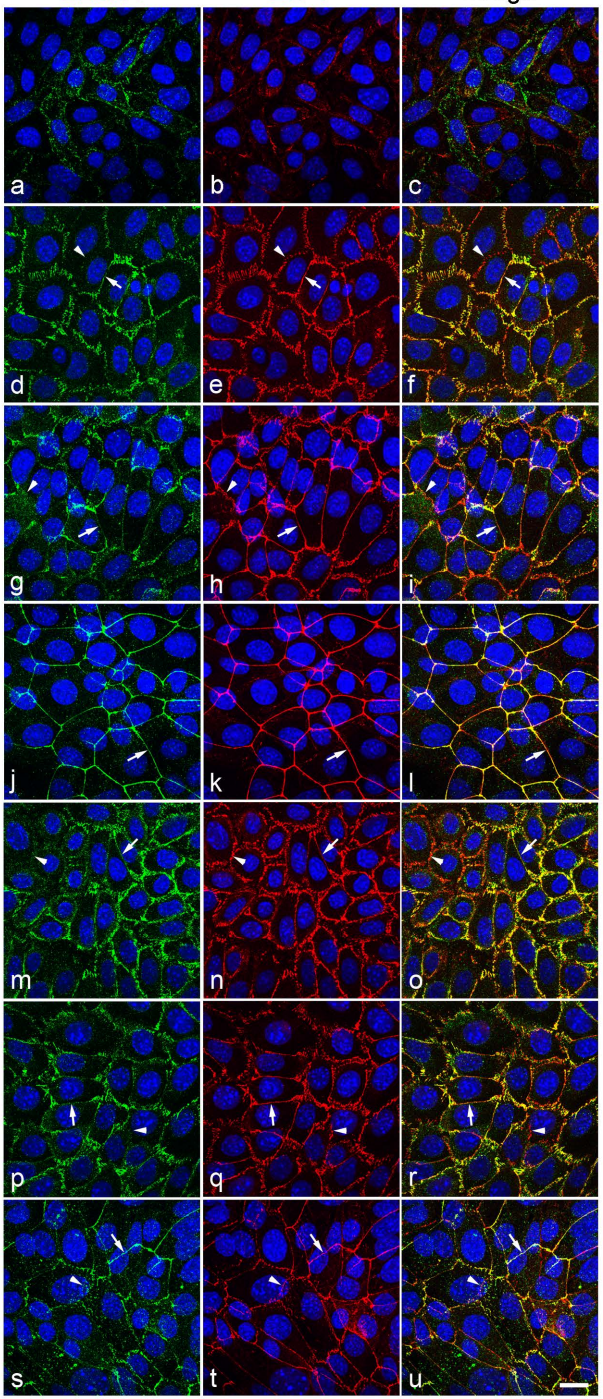
CLDN4
ZO-1
merge
0 h
Ca, 2 h
Ca, 6 h
Ca, 12 h
Ca+AM, 2 h
Ca+AM, 6 h
Ca+AM, 12 h
a
b
c
d
e
f
g
h
i
j
k
l
m
n
o
p
q
r
s
t
u

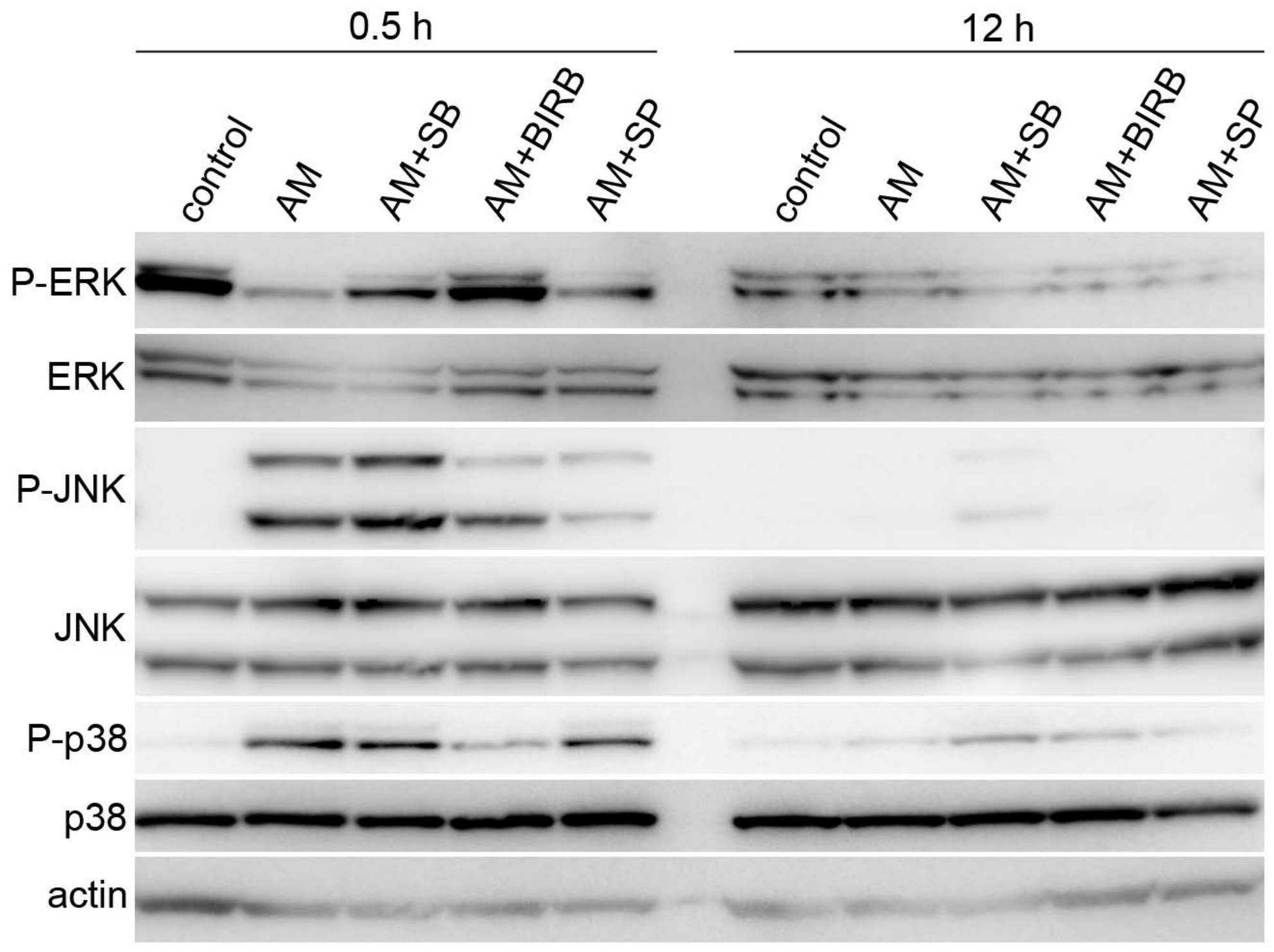
0.5 h
12 h
control
AM
AM+SB
AM+BIRB
AM+SP
control
AM
AM+SB
AM+BIRB
AM+SP
P-ERK
ERK
P-JNK
JNK
P-p38
p38
actin

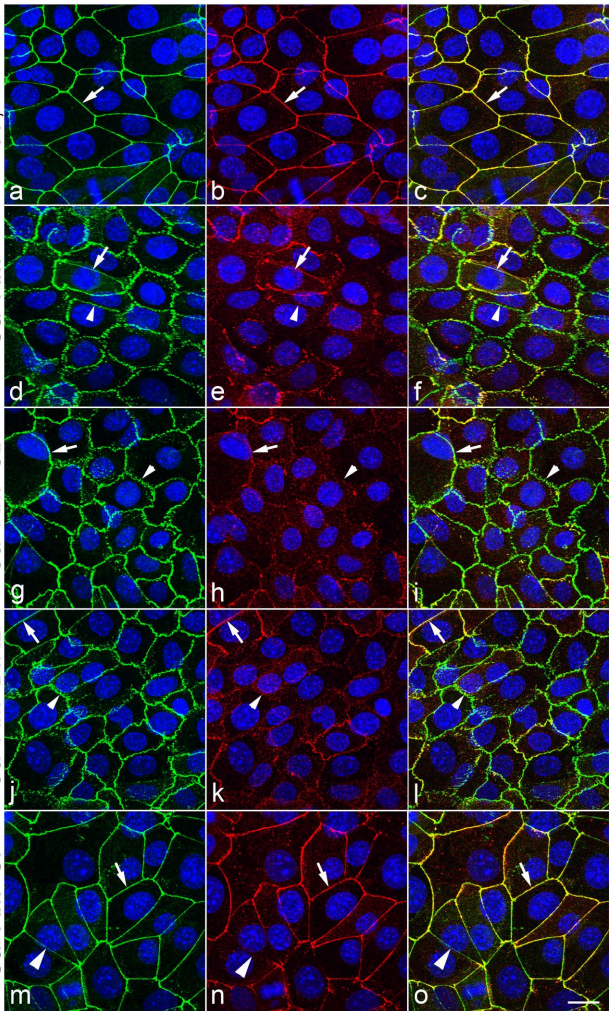
ZO-1
CLDN4
merge
Ca, 12 h
Ca+AM
Ca+AM+SB
Ca+AM+BIRB
Ca+AM+SP
a
b
c
d
e
f
g
h
i
j
k
l
m
n
o

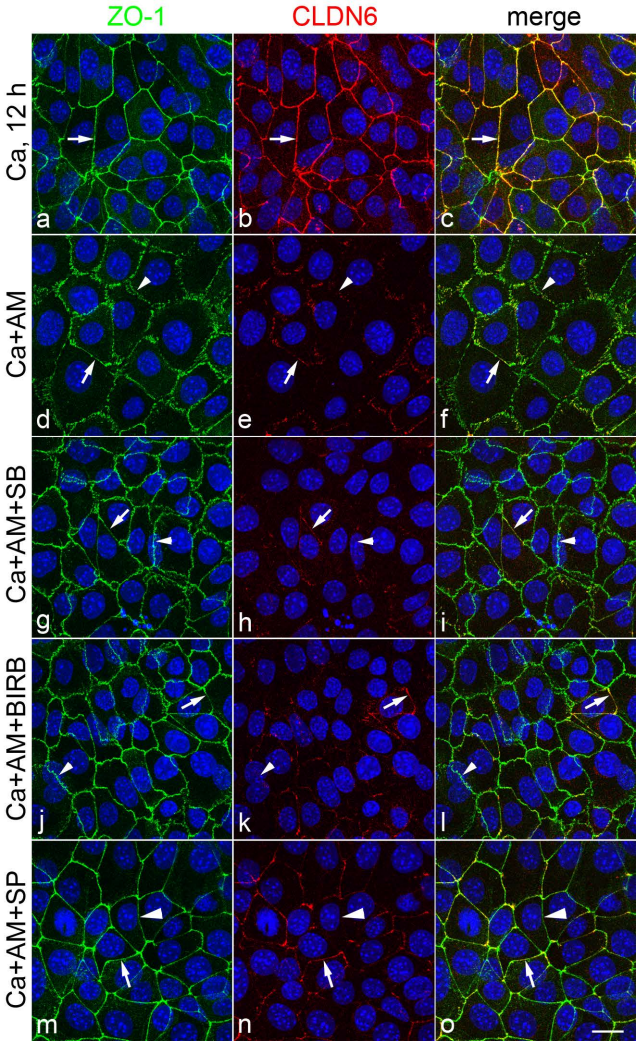
ZO-1
CLDN6
merge
Ca, 12 h
Ca+AM
Ca+AM+SB
Ca+AM+BIRB
Ca+AM+SP
a
b
c
d
e
f
g
h
i
j
k
l
m
n
o

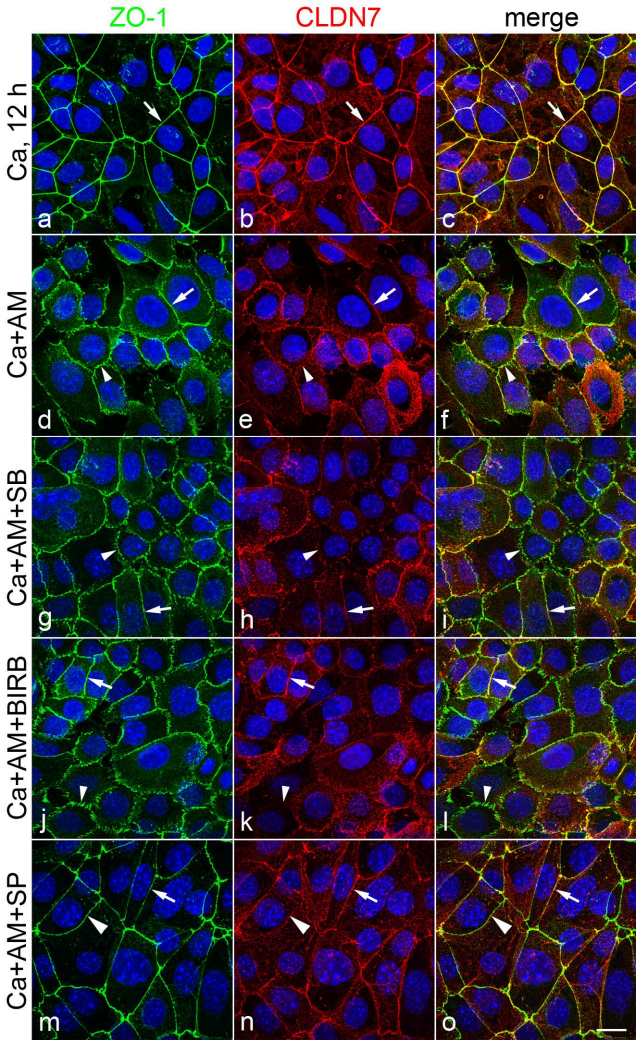
ZO-1
CLDN7
merge
Ca, 12 h
Ca+AM
Ca+AM+SB
Ca+AM+BIRB
Ca+AM+SP
a
b
c
d
e
f
g
h
i
j
k
l
m
n
o

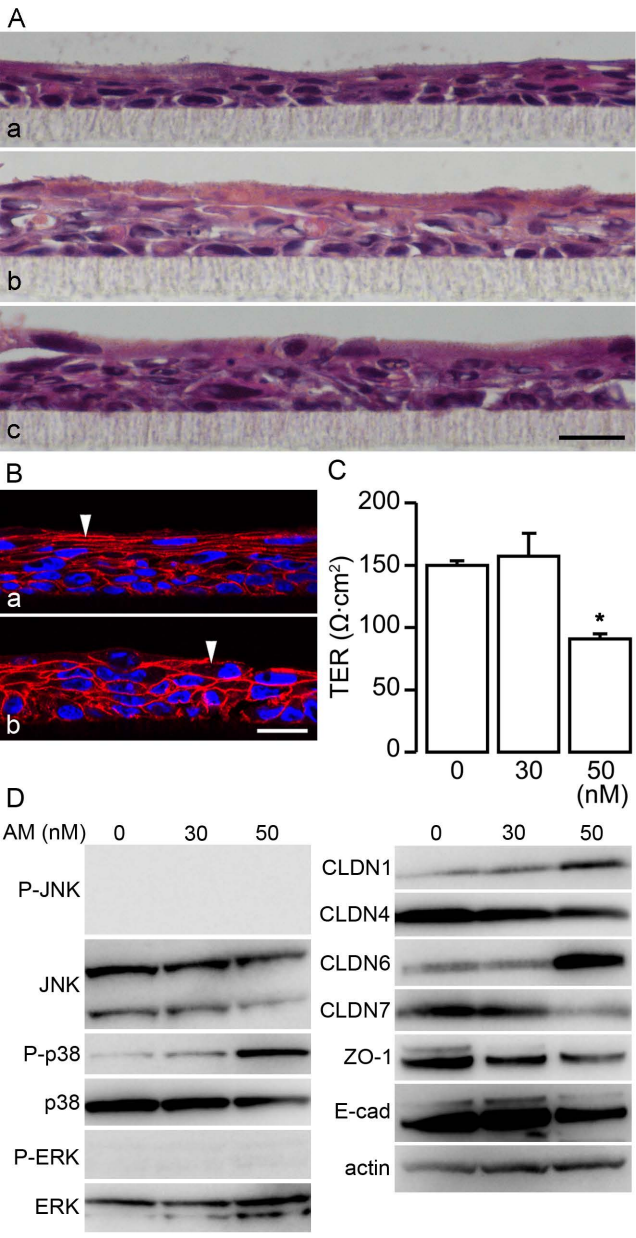
A
a
b
c
B
a
b
C
200
150
100
50
0
TER (Ω·cm²)
*
0
30
50
(nM)
D
AM (nM)
0
30
50
P-JNK
JNK
P-p38
p38
P-ERK
ERK
0
30
50
CLDN1
CLDN4
CLDN6
CLDN7
ZO-1
E-cad
actin

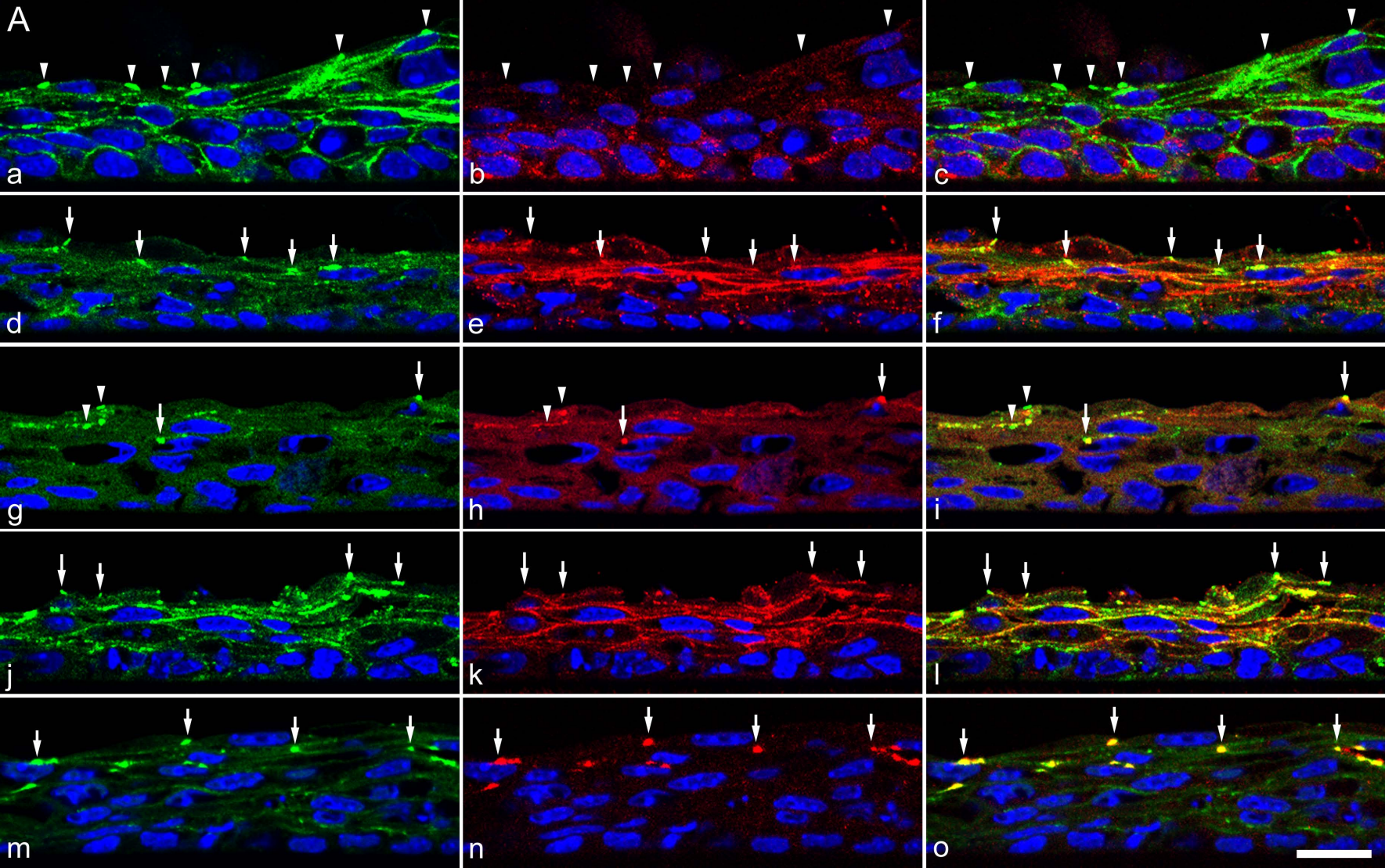
A
a
b
c
d
e
f
g
h
i
j
k
l
m
n
o

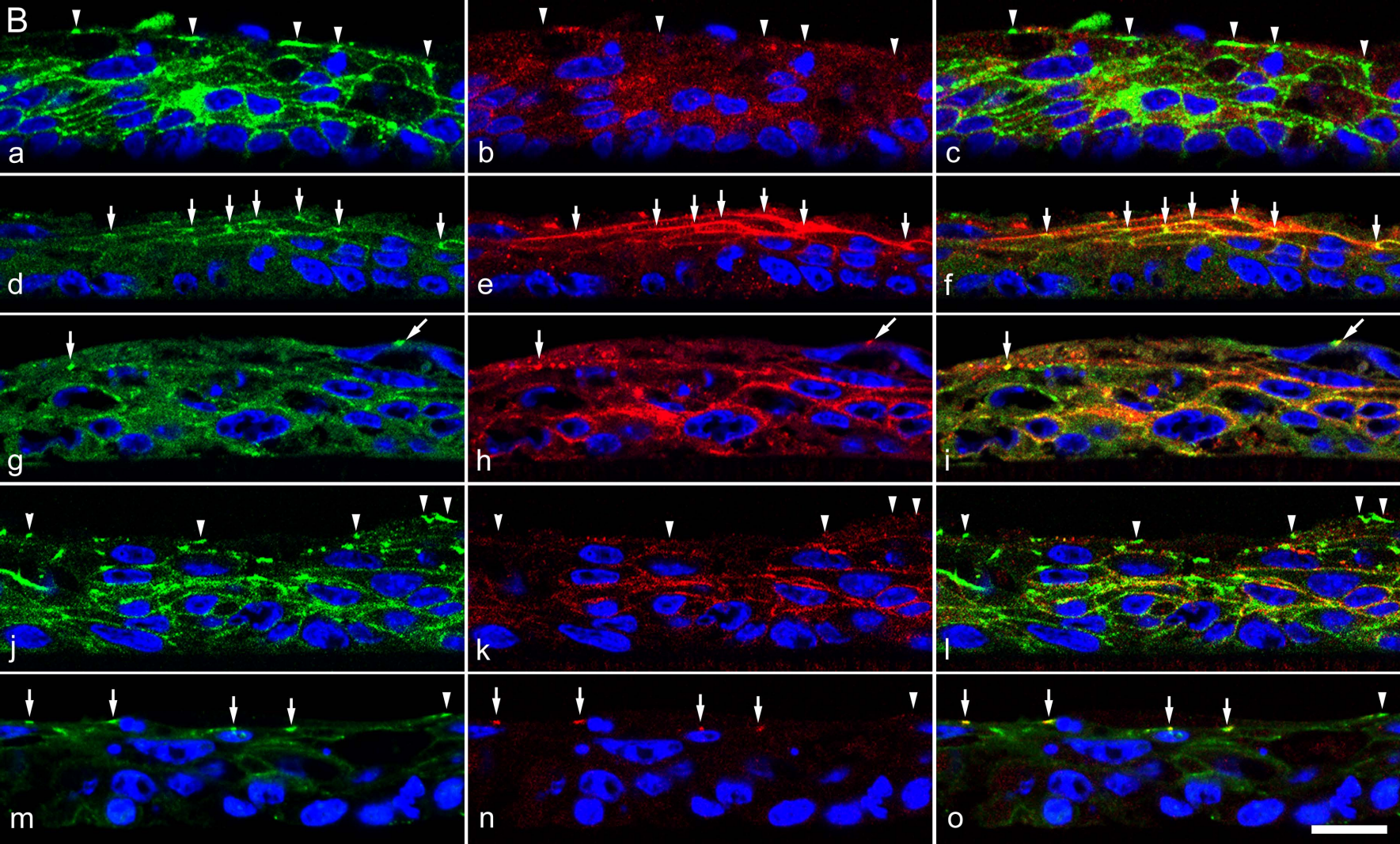
B
a
b
c
d
e
f
g
h
i
j
k
l
m
n
o

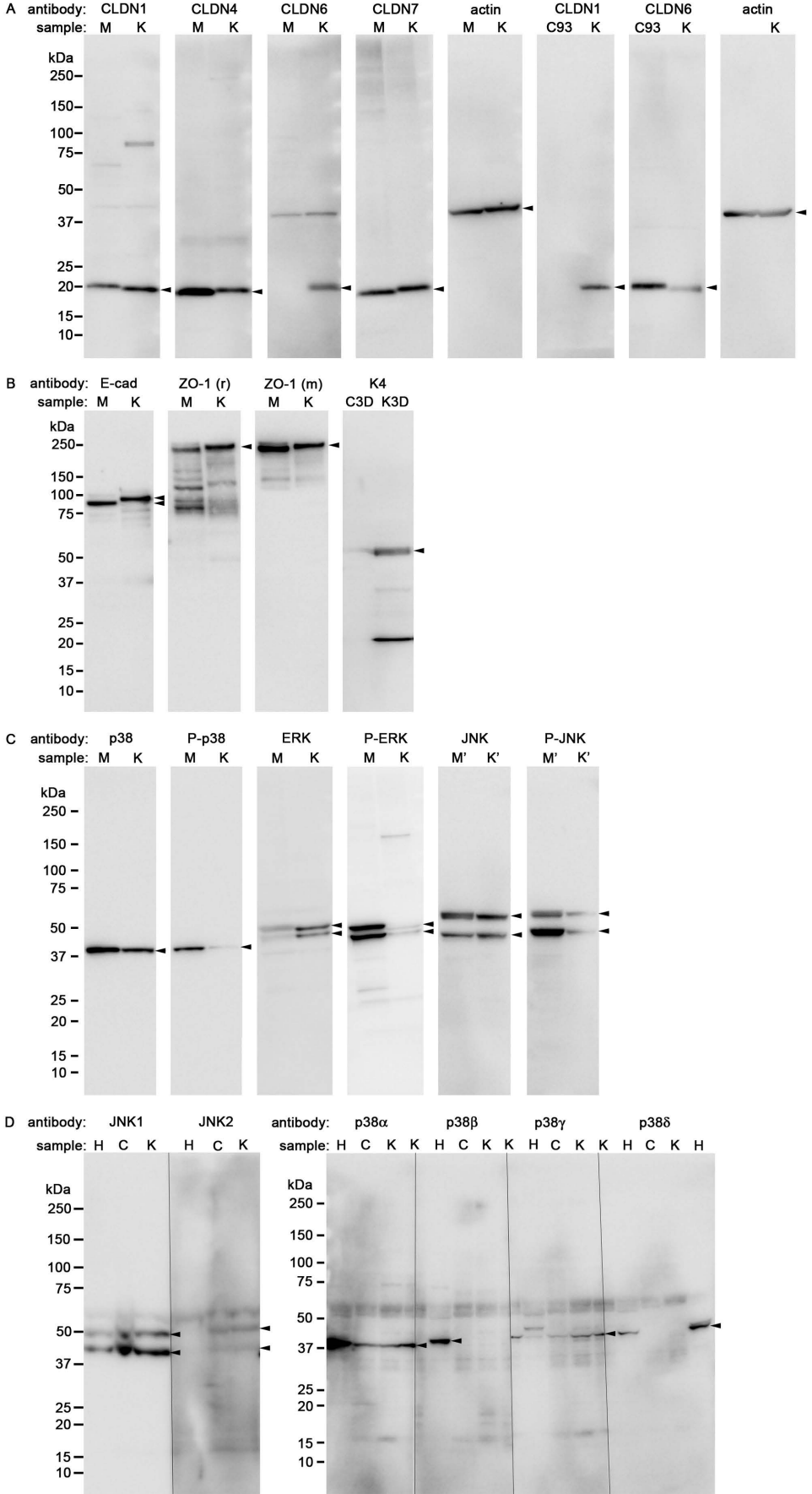
A
antibody: CLDN1 CLDN4 CLDN6 CLDN7 actin CLDN1 CLDN6 actin
sample: M K M K M K M K M K C93 K C93 K K
kDa
250
150
100
75
50
37
25
20
15
10
B
antibody: E-cad ZO-1 (r) ZO-1 (m) K4
sample: M K M K M K C3D K3D
kDa
250
150
100
75
50
37
25
20
15
10
C
antibody: p38 P-p38 ERK P-ERK JNK P-JNK
sample: M K M K M K M K M' K' M' K'
kDa
250
150
100
75
50
37
25
20
15
10
D
antibody: JNK1 JNK2
sample: H C K H C K
kDa
250
150
100
75
50
37
25
20
15
10
antibody: p38α p38β p38γ p38δ
sample: H C K K H C K K H C K K H C K H
kDa
250
150
100
75
50
37
25
20
15
10

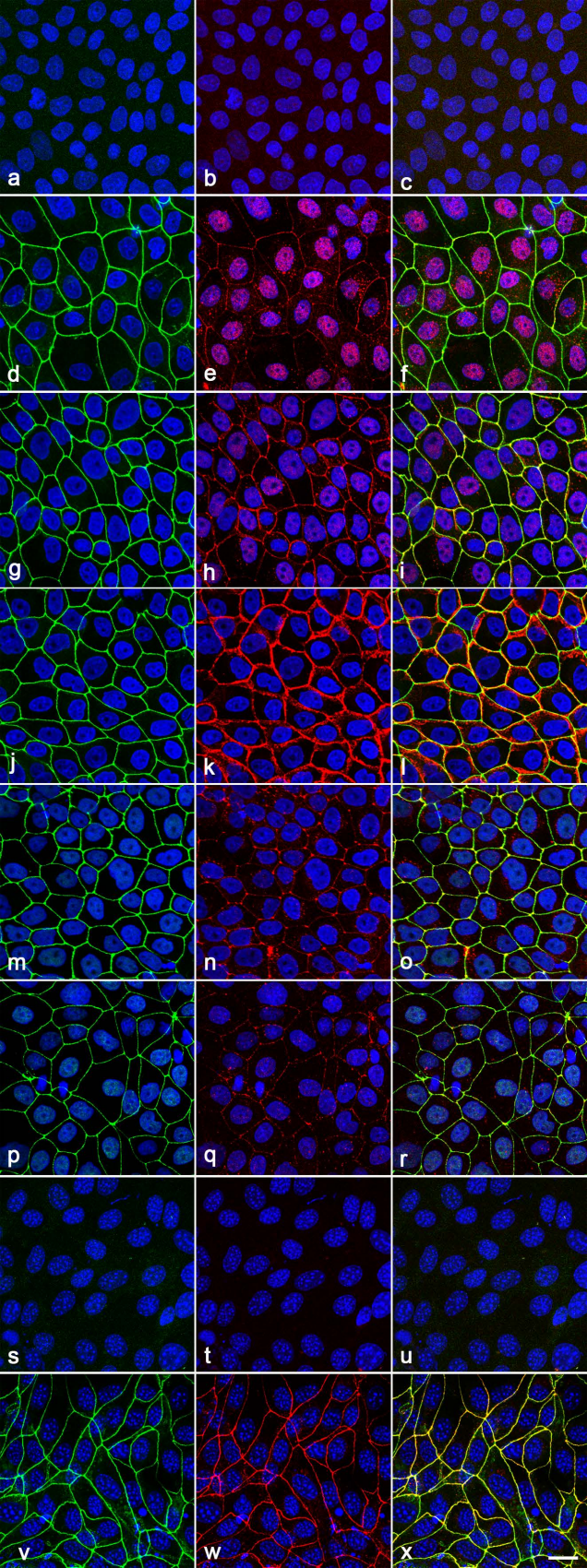
a
b
c
d
e
f
g
h
i
j
k
l
m
n
o
p
q
r
s
t
u
v
w
x

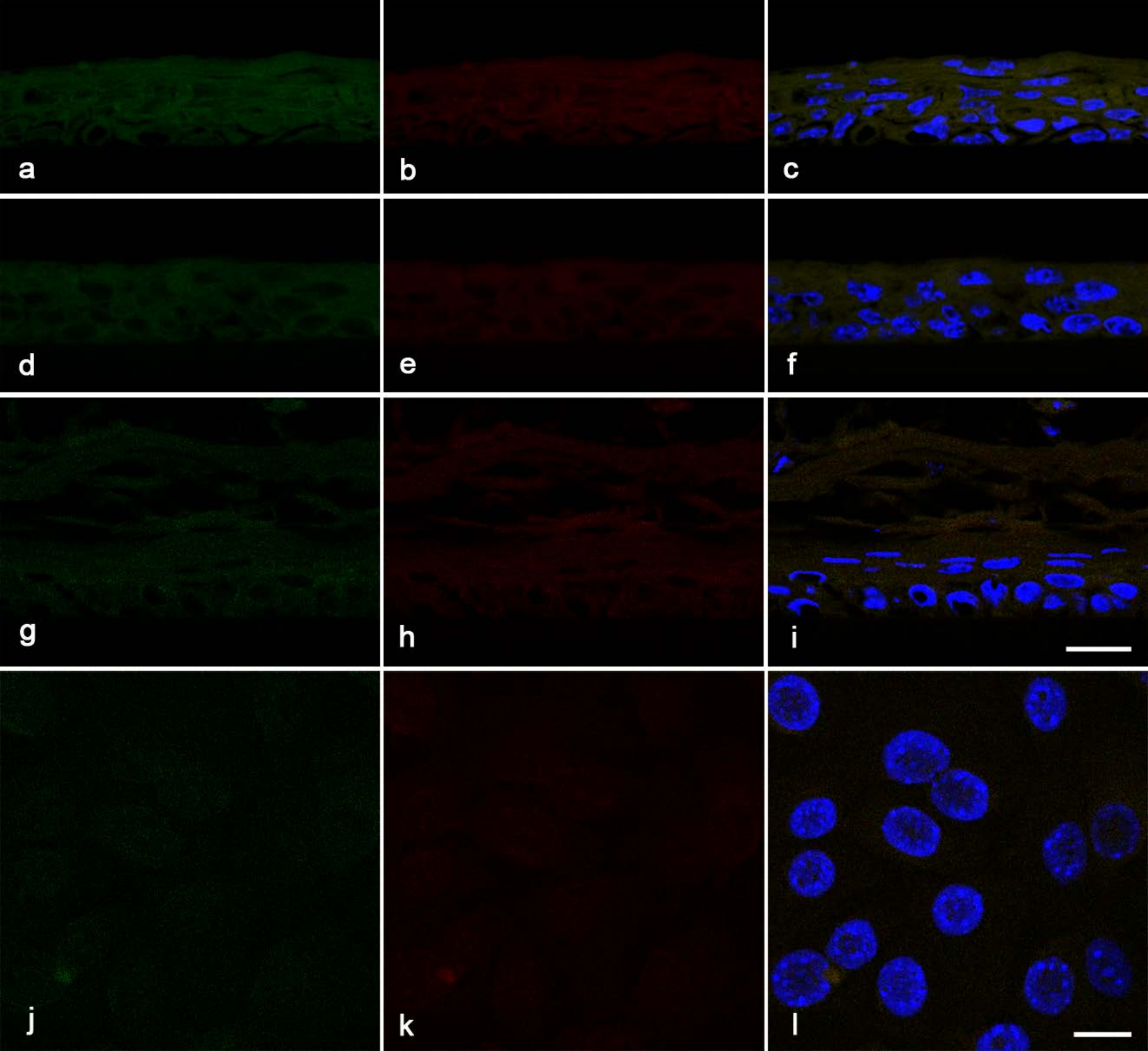
a
b
c
d
e
f
g
h
i
j
k
l

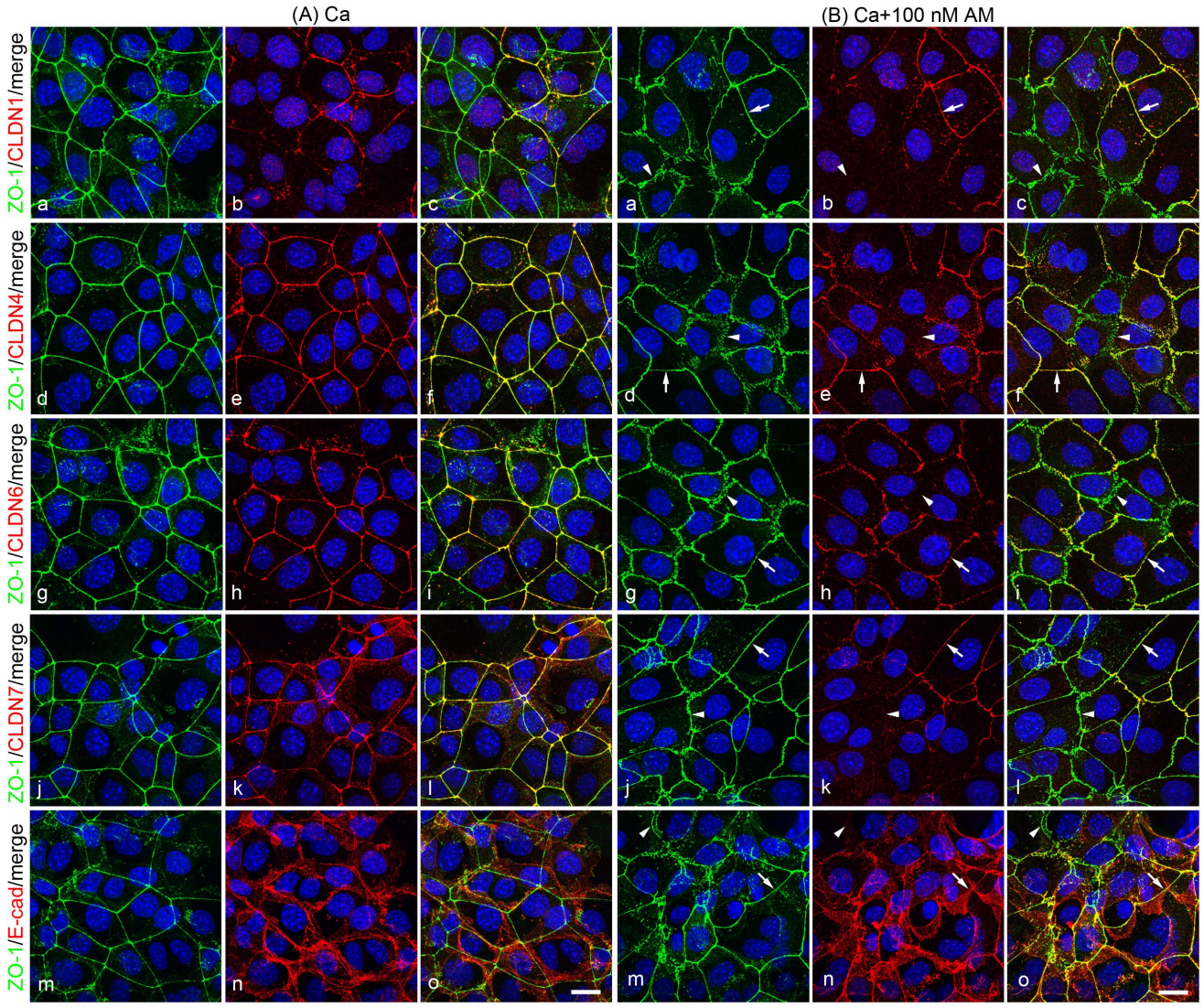
(A) Ca
(B) Ca+100 nM AM
ZO-1/CLDN1/merge
ZO-1/CLDN4/merge
ZO-1/CLDN6/merge
ZO-1/CLDN7/merge
ZO-1/E-cad/merge
a
b
c
d
e
f
g
h
i
j
k
l
m
n
o